Filomat 35:14 (2021), 4837–4870
https://doi.org/10.2298/FIL2114837S

Published by Faculty of Sciences and Mathematics,
University of Niš, Serbia
Available at: http://www.pmf.ni.ac.rs/filomat

Effect of Anti-Predator Behaviour in a Prey-Predator System with Strong Allee Effect in Prey Population

Sangeeta Saha[a], G. P. Samanta[a]

[a]*Department of Mathematics, Indian Institute of Engineering Science and Technology, Shibpur, Howrah - 711103, INDIA*

Abstract. In this work a predator-prey model is proposed where prey species shows anti-predator behaviour to save themselves from predator's attack. Moreover, a strong Allee effect has been introduced in the prey population to make the model more realistic to the environment. Both generalist and specialist predators have been taken to observe the system dynamics minutely. The predator population decreases with increasing value of 'rate coefficient of anti-predator behaviour' when generalist predator is considered but in presence of the specialist predator, the predator population first increases up to a threshold value and then decreases. It means a very small rate of anti-predation does not affect the predator's growth very much but if prey attacks the predator at a larger rate, then the predator population decreases. Also, the existence of one dimensional and two-dimensional bifurcations have been observed by making different parameters as bifurcating parameters around the steady states.

1. Introduction

The relationship between predators and their prey population has become an important topic in theoretical ecology and Lotka-Volterra system first developed the ground work on this topic. In this context it is mentioned that researchers have analyzed predator-prey systems by refining the Lotka-Volterra model to get new results [6, 15, 20, 35, 45]. Although in most of the cases, researchers assume that prey is always consumed by the predator but real-world scenarios sometimes contradict this assumption as predators may be harmed by their prey [23, 34]. So, anti-predator behaviour, i.e., role reversal process between prey and predator often occur in the environment. Prey population develop some evolutionary adaptation over time to fight back against predator and it is called anti-predator behaviour. Many animals use claws, horns, teeth etc. to fight with the predators and this is, in fact, a kind of anti-predator behaviour. There are many research works have already been done on this type of behaviour [5, 7, 25]. Some of the works are dealt with the assumption that prey applies the anti-predator strategies to avoid predation only [8, 10, 14, 32] but some literature consider that preys can even attack predators (especially juvenile predators) [3, 9, 19]. From the work of Lingle and Pellis [19], it is observed that mule deer (*O. hemionus*) stand against their predator coyote (*Canis latrans*) at the time of being attacked or encountered and defend their conspecifics

2020 *Mathematics Subject Classification*. Primary 92B05; Secondary 92D25, 92D40
Keywords. Ecosystems; Allee effect; Generalist and Specialist predator; Anti-predator behaviour; Bifurcations
Received: 13 August 2020; Revised: 10 September 2020; Accepted: 20 September 2020
Communicated by Maria Alessandra Ragusa
Corresponding author: G. P. Samanta
Research supported by University Grants Commission, India
Email addresses: sangeetasaha629@gmail.com (Sangeeta Saha), g_p_samanta@yahoo.co.uk, gpsamanta@math.iiests.ac.in (G. P. Samanta)

by attacking the predators. Ford and Reeves [9], in their experiment, observed that a group of five or six baleen whales (*Mysticeti*) adopt some fight (or, defence) strategies when attacked by killer whales and these strategies include self-defence, defence of calves by their mothers and even group defence of whales. Let us take another biological reference where prey species indirectly reduce its predator density. In China, alpine meadow is one of the important ecosystems as it regulates some basic ecological amenities like maintenance of biodiversity, purification of water, soil and vegetation generation and renewal, decomposition of waste materials etc. But according to statistical reports, for the past few years, many alpine meadows have been degraded which affect the ecology as well as economy [41, 43, 44]. Due to this degradation, species diversity and vegetation cover have been reduced which causes commodity scarcity, dust storms etc. There is a small mammal named plateau pika (*Ochotona curzoniae*) which is a prime species in this alpine meadow ecosystem. It is observed that plateau pika is in high density in a degraded ecosystem and it is considered as a pest which needs to be controlled [17, 30]. In alpine meadow ecosystem, plateau pika feeds on the vegetation and a lot of soil is thrown out when a plateau pika digs a hole and piles up a heap. But this heap block the growth of existing vegetation and in fact, no vegetation can grow on the mound for a long time due to unfavourable climate. As a result, the area for growth of vegetation reduces resulting in a reduction of vegetation [42]. But the interesting part is increased density of vegetation makes a negative impact on plateau pika. If a plateau pika is provided with higher vegetation, they become negligent about their predators like tibetan fox etc. and hence are caught easily [29]. That means, plateau pika is indirectly decreased by the high volume of vegetation.

According to experimental results, anti-predator behaviour of prey species is observed in terms of either (i) morphological changes or through changes in behaviour [18, 22, 27, 37] or (ii) attack of prey population on their predators [3, 13, 28]. Though anti-predator behaviour is a natural phenomenon, few works have been done on this topic [1, 12, 26]. Ives and Dobson [12] modelled a predator-prey system with anti-predator behaviour through morphological changes (i.e., (i)) with the following equations:

$$\dot{x}(t) = \lambda x\left(1 - \frac{x}{k}\right) - \nu - \frac{e^{-\epsilon\nu}qxy}{1+ax}, \quad \dot{y}(t) = \frac{ce^{-\epsilon\nu}qxy}{1+ax} - my$$

where $x(t)$, $y(t)$ are respectively prey and predator densities at time t. The parameters ν and ϵ are positive constants which denote prey's involvement in anti-predator behaviour and efficiency of the anti-predator behaviour respectively. So, the predation rate decreases with an increase of either or both of ν and ϵ. Their results show that the anti-predator behaviour of prey species can increase the density of the prey population and reduce the probability of occurrence of damped oscillations. Again for the second case (i.e., (ii)), adult prey is often invulnerable to their predators and they can even kill the juveniles predators.

W. C. Allee, in 1931, observed a relationship between the density and average fitness of the individuals in a population which is defined as Allee effect [2, 4]. Under Allee effect, per capita growth rate of a population increases and reaches to a maximum value which lies below of the carrying capacity. So, for low population density, the growth rate first increases until it reaches a maximum and then starts to decrease. Allee effect mainly occurs due to different reasons such as the lower probability of successful mating, difficulties in finding mates, predator avoidance because of environmental condition, cooperative defence etc. Two types of Allee effect can be observed depending on depletion of per capita growth at low population density: strong Allee effect [16, 38, 40] and weak Allee effect [31, 39]. For the case of strong Allee effect, per capita growth rate of a population becomes negative at low population density, i.e., the species extinct below of a threshold value. But for weak Allee effect, there is no such threshold below which the population extinct and here per capita growth rate is low at low population density. The growth rate of plants, as well as animals, often affect by Allee effect. Confused flour beetles (*Tribolium confusum*) is one of the most injurious insect pests for grain products which is used to demonstrate the Allee effect first. Also, pollinators got attracted towards the small dispersed patches in fig trees (*Fiscus sp.*) which affect pollination [4]. Moreover, different types of Allee effects have been seen in African wild dogs (*Lycaon pictus*), kakapo birds (*Strigops habroptilus*) etc.

There are some published works in the literature where anti-predator behaviour is considered in prey population. Tang and Xiao, in 2015, have proposed a prey-predator model with anti-predator behaviour where the adult prey can attack exposed predators [36]. They have concluded that the anti-predator

behaviour of the prey population resists the aggression of a predator species. Again, Sun et. al. in their work have considered a predator-prey system where anti-predator behaviour of prey species occurs only when the prey population exceeds a threshold value [33]. They have concluded that higher anti-predator rate induces persistence of the prey population and also the coexistence depends on the anti-predator behaviour. A higher value of anti-predator behaviour rate coefficient helps to coexist both the prey and predator populations and also damps the predator-prey oscillations. Till now, there is no work has been done on anti-predator behaviour of prey population in presence of Allee effect. So, we, in this work, have modelled a prey-predator system where prey species shows anti-predator behaviour to avoid a high rate of attack of the predator in presence of strong Allee effect. Also, not only the specialist predator but also generalist predator is considered in a separate model to analyse the results of how anti-predator behaviour affect the growth of the predator population in both cases.

The complexity of any model can be manipulated by appropriate choice of functional responses. In our work, we have shown that the inclusion of some relevant biological arguments has made the model system more realistic. Firstly, both the generalist and specialist predator have been considered here. There are only a few species exist in the environment which are considered as specialist predators. Moreover, a prey-predator interaction with generalist predator can show more biologically relevant properties as the extinction of predator does not fully depend on the extinction of prey and predator can survive without consuming this particular prey. So, the main purpose of this literature is to model a prey-predator interaction with anti-predator behaviour in presence of strong Allee effect to observe its impact on the dynamics. This paper is organized as follows: Section 2 contains the mathematical models for both generalist and specialist predator. Section 3 shows that all the populations are positive and bounded. Extinction criterion for the populations have been stated in section 4 and equilibria with their existence for both models are described in section 5. Section 6 proves that some of the equilibrium points are locally asymptotically stable under some parametric restrictions. Conditions for the occurrence of local bifurcation around the equilibria are discussed in section 7. Figures in section 8 support the analytical findings. The work has ended up with a brief discussion about the system dynamics.

2. Mathematical Model: Basic Equations

An ecological system in terms of mathematical equations mainly provide the proper insight of the system and it becomes easier to find the dynamics of the model with time. Our main purpose of this study is to model the prey-predator interaction where prey population exhibits anti-predator behaviour. In this study, we have highlighted the complex and rich dynamics induced by the prey dependent anti-predator behaviour.

The system is a two species food chain model consists of a prey population (X) and a predator population (Y). It is assumed that when there is no predator present in the system, prey population grows according to logistic law with intrinsic growth rate r_1 and carrying capacity K_1. The parameter K_0 represents the Allee threshold of prey population in absence of predator with the condition $0 < K_0 << K_1$. The parameter M represents the predation rate coefficient of predator on prey species and as the hunting procedure is not instantaneous, let T_h be the average handling time of predator for each prey. So, the predation between prey and predator follows Holling type-II functional response. First the predator is suggested to be a generalist one where the alternative food supply is available. It is quite obvious as predators can often prefer a different number of prey for consumption. In the absence of this prey species, it is assumed that the predator grows logistically with intrinsic growth rate r_2 and carrying capacity K_2. If the predator is assumed to be specialist one, then the predator live depending on only one particular prey species. In that case, let, c be the biomass conversion rate. The parameter η_1 denotes the rate of anti-predator behaviour of prey species to the predator population. It is observed that such behaviour does not benefit the prey population directly but only reduces the growth of the predator population [3].

So, for generalist predator, considering all these assumptions, we get the system as:

$$\begin{aligned}\frac{dX(T)}{dT} &= r_1X\left(1-\frac{X}{K_1}\right)\left(\frac{X}{K_0}-1\right)-\frac{MXY}{1+T_hMX},\ \ X(0)>0,\\ \frac{dY(T)}{dT} &= r_2Y\left(1-\frac{Y}{K_2}\right)-\eta_1XY,\ \ Y(0)>0.\end{aligned} \tag{2.1}$$

Using the scaling $x=\frac{X}{K_1}$, $y=\frac{Y}{K_2}$ and $t=\frac{r_1K_1}{K_0}T$, system (2.1) becomes

$$\begin{aligned}\frac{dx(t)}{dt} &= x(1-x)(x-p)-\frac{mxy}{1+ax},\ \ x_0=x(0)>0,\\ \frac{dy(t)}{dt} &= ry(1-y)-\eta xy,\ \ y_0=y(0)>0,\end{aligned} \tag{2.2}$$

where $p=\frac{K_0}{K_1}$, $m=\frac{MK_2K_0}{K_1}$, $a=T_hMK_1$, $r=\frac{r_2K_0}{r_1K_1}$, $\eta=\frac{\eta_1K_0}{r_1}$.
And, when the predator is specialist one, the model becomes:

$$\begin{aligned}\frac{dX(T)}{dT} &= r_1X\left(1-\frac{X}{K_1}\right)\left(\frac{X}{K_0}-1\right)-\frac{MXY}{1+T_hMX},\ \ X(0)>0,\\ \frac{dY(T)}{dT} &= \frac{cMXY}{1+T_hMX}-DY-\eta_1XY,\ \ Y(0)>0.\end{aligned} \tag{2.3}$$

Using the scaling $x=\frac{X}{K_1}$, $y=\frac{Y}{K_1}$ and $t=\frac{r_1K_1}{K_0}T$, we get system (2.3) as

$$\begin{aligned}\frac{dx(t)}{dt} &= x(1-x)(x-p)-\frac{m_1xy}{1+ax},\ \ x_0=x(0)>0,\\ \frac{dy(t)}{dt} &= \frac{cm_1xy}{1+ax}-dy-\eta xy,\ \ y_0=y(0)>0,\end{aligned} \tag{2.4}$$

where $p=\frac{K_0}{K_1}$, $m_1=\frac{MK_0}{r_1}$, $a=T_hMK_1$, $d=\frac{DK_0}{r_1K_1}$, $\eta=\frac{\eta_1K_0}{r_1}$. Here all model parameters r_1, K_0, K_1, r_2, M, c, D, T_h, K_2, η are positive constants.

3. Positivity and Boundedness

This section shows that the variables of system (2.2) and (2.4) remain positive and bounded for all time.

Theorem 3.1. *Solutions of systems (2.2) and (2.4) starting in $\mathbb{R}^2_+$ are positive for all time.*

Proof. Right hand sides of systems (2.2) and (2.4) are continuous and locally Lipschitzian on C (space of continuous functions) and hence solutions $(x(t), y(t))$ of (2.2) as well as (2.4) exist and are unique on the interval $[0, \tau)$, where $0 < \tau \leq +\infty$ [11]. From the first equation of (2.2), we get

$$\frac{dx(t)}{dt} = x(1-x)(x-p)-\frac{mxy}{1+ax},$$

$$\text{i.e., } x(t) = x_0\exp\left[\int_0^t\left\{(1-x(s))(x(s)-p)-\frac{my(s)}{1+ax(s)}\right\}ds\right] > 0, \text{ for } x_0>0.$$

First equation of system (2.4) is same as of system (2.2) and so $x(t) > 0$ holds for the later one too. Again from the second equation of (2.2):

$$y(t) = y_0\exp\left(\int_0^t\{r(1-y(s))-\eta x(s)\}\,ds\right) > 0, \text{ for } y_0>0.$$

Similarly, from the second equation of (2.4), we get

$$y(t) = y_0 \exp\left(\int_0^t \left\{\frac{cm_1x(s)}{1+ax(s)} - d - \eta x(s)\right\} ds\right) > 0, \text{ for } y_0 > 0.$$

□

Theorem 3.2. *Solutions of system* (2.2) *starting in* $\mathbb{R}^2_+$ *remain uniformly bounded for all time.*

Proof. **Case I:** Let $x_0 \leq 1$. Claim: $x(t) \leq 1$.
Suppose, it in not true. Then, $\exists$ t_1 and t_2 such that $x(t_1) = 1$ and $x(t) > 1$, $\forall\, t \in (t_1, t_2)$. Here '$\exists$' stands for the words 'there exists', '$\forall$' stands for 'for all' and '$\in$' stands for 'belongs to'. So, from the first equation of (2.2): $\forall\, t \in (t_1, t_2)$,

$$x(t) = x_0 \exp\left(\int_0^t \phi(x(s), y(s))\, ds\right)$$

where, $\phi(x(s), y(s)) = (1 - x(s))(x(s) - p) - \frac{my(s)}{1+ax(s)}$

$$\begin{aligned}\text{So, } x(t) &= x_s(0) \exp\left[\left(\int_0^{t_1} \phi(x(s), y(s))\, ds\right) + \left(\int_{t_1}^{t} \phi(x(s), y(s))\, ds\right)\right] \\ &= x(t_1) \exp\left(\int_{t_1}^{t} \phi(x(s), y(s))\, ds\right) \\ &= \exp\left(\int_{t_1}^{t} \phi(x(s), y(s))\, ds\right)\end{aligned}$$

As, $0 < p < 1$, it gives, $\phi(x, y) < 0$
So, $x(t) < 1$, which is a contradiction.
Case II: Let $x_0 > 1$; our claim is: $\limsup_{t\to\infty} x(t) \leq 1$.
If it is not true, then $x(t) > 1\ \forall\, t > 0$; i.e. $\phi(x, y) < 0$.

$$\text{So, } x(t) = x_0 \exp\left(\int_0^t \phi(x(s), y(s))\, ds\right) < x_0.$$

From the first equation of (2.2):

$$\frac{dx}{dt} < (\underline{x} - p)x(1 - x), \text{ where } \underline{x} = \liminf_{t\to\infty} x(t)$$

$$\Rightarrow \limsup_{t\to\infty} x(t) \leq 1.$$

Moreover from the 2^{nd} equation of (2.2) we have

$$\frac{dy}{dt} = ry(1 - y) - \eta xy \ \leq ry(1 - y)$$

$\Rightarrow \limsup_{t\to\infty} y(t) \leq 1$.
Hence, the solutions of system (2.2) will enter into region:

$$\Omega_1 = \{(x, y) : 0 \leq x(t) \leq 1; 0 \leq y(t) \leq 1\}.$$

□

Theorem 3.3. *Solutions of system* (2.4) *starting in* $\mathbb{R}^2_+$ *remain uniformly bounded for all time.*

Proof. 1^{st} equation of system (2.4) is: $\frac{dx}{dt} = x(1-x)(x-p) - \frac{m_1xy}{1+ax}$
Proceeding as Theorem 3.2, we have $\limsup_{t\to\infty} x(t) \leq 1$.
Consider $\rho = \frac{(p+1)}{3} + \frac{\sqrt{3(p-1)^2+(p+1)^2+12}}{6}$.
Let $W = Ax(t) + By(t)$, where $A = \frac{1}{2\rho^2\left(\rho - \frac{(p+1)}{2}\right)}$ and $B = \frac{1}{c}$.

$$\text{So, } \frac{dW}{dt} = A\frac{dx}{dt} + B\frac{dy}{dt} = A\left[x(1-x)(x-p)+x\right] - Ax - \frac{d}{c}y - \eta xy$$
$$\leq A\left[x(1-x)(x-p)+x\right] - Ax - \frac{d}{c}y$$

Let $H = x(1-x)(x-p)+x$. Then G attains its maximum value at $x = \rho$ and $H_{max} = \frac{1}{A}$.

$$\text{So, } \frac{dW}{dt} \leq 1 - \tau W, \text{ where } \tau = \min\{A, d\}.$$
$$\text{Then, } W(t) \leq \frac{1}{\tau} + W(x_0, y_0)\exp(-\tau t)$$
$$\Rightarrow \lim_{t\to\infty} W(t) \leq \frac{1}{\tau}.$$

Therefore, all solutions of system (2.4 enter into the region:

$$\Omega_2 = \left\{(x,y) : 0 \leq x(t) \leq 1; 0 \leq W(t) \leq \frac{1}{\tau} + \epsilon, \epsilon > 0\right\}.$$

□

4. Extinction Scenarios

Theorems in this section provide the criterion for which prey and predator extinct from the system in long run.
Let us denote the following notations: $\overline{x} = \limsup_{t\to\infty} x(t)$; $\overline{y} = \limsup_{t\to\infty} y(t)$. Similarly, $\underline{x} = \liminf_{t\to\infty} x(t)$; $\underline{y} = \liminf_{t\to\infty} y(t)$.

4.1. Considering Generalist predator:

Here we use the facts that $\overline{x} \leq 1$ and $\overline{y} \leq 1$.
First two theorems give the extinction criterion of prey species and the last one provide the criterion for predator extinction.

Theorem 4.1. *If* $\overline{x} < p$, *then* $\lim_{t\to\infty} x = 0$.

Proof. Choose ϵ s.t. $0 < \epsilon < p - \overline{x}$, then $\exists\, T > 0$ s.t. $x(t) < \overline{x} + \epsilon$, $\forall t > T$.
for $t > T$:

$$\frac{dx}{dt} = x\left[(1-x)(x-p) - \frac{my}{1+ax}\right]$$
$$\leq x(1-x)(x-p)$$
$$\leq x(\overline{x} + \epsilon - p)$$
$$= -\mu x \quad [\text{where, } \mu = (p - \overline{x} - \epsilon) > 0]$$

Hence, $\lim_{t\to\infty} x = 0$. □

Remark 4.2. *So, it is concluded that only the Allee effect can wash out the prey population. If prey species stay below the Allee threshold, then they can not live in the system and goes extinct with time.*

Theorem 4.3. *If* $m\underline{y} > (p+2)(1+a)$, *then* $\lim_{t\to\infty} x = 0$.

Proof. Choose ϵ such that for $0 < \epsilon < 1-p$, $\exists\ T_1 > 0$, s.t. $x(t) < 1+\epsilon,\ \forall\, t > T_1$.
Also, be definition, for $0 < \epsilon_1 < \underline{y} - \dfrac{(p+2)(1+a)}{m}$, $\exists\ T_2 > 0$, s.t. $y(t) > \underline{y} - \epsilon_1,\ \forall\, t > T_2$.
For $\forall\, t > \max\{T_1, T_2\}$:

$$\begin{aligned}
\frac{dx}{dt} &= x\left[(1-x)(x-p) - \frac{my}{1+ax}\right] \\
&\le x\left[(1+p)(1+\epsilon) - p - \frac{m(\underline{y}-\epsilon_1)}{1+a}\right] \\
&\le -x\left[\frac{m(\underline{y}-\epsilon_1)}{1+a} - (p+2)\right] \\
&= -\left(\frac{m}{1+a}\right)\left[\underline{y} - \epsilon_1 - \frac{(p+2)(1+a)}{m}\right]x \\
&= -\mu\left(\frac{m}{1+a}\right)x, \ \left[\text{where } \mu = \underline{y} - \epsilon_1 - \frac{(p+2)(1+a)}{m} > 0\right] \\
&= -Ux, \ \left[\text{where } U = \mu\left(\frac{m}{1+a}\right)\right]
\end{aligned}$$

Hence, $\lim_{t\to\infty} x = 0$. □

Remark 4.4. *If the predator starts to consume prey population with a higher rate, then the prey biomass decreases gradually with time. This leads to the declination and ultimately extinction of prey population from the system with time.*

Theorem 4.5. *If* $\eta\underline{x} > r$, *then* $\lim_{t\to\infty} y(t) = 0$.

Proof. Choose ϵ such that for $0 < \epsilon < \underline{x} - \frac{r}{\eta}$, $\exists\ T > 0$, s.t. $x(t) > \underline{x} - \epsilon,\ \forall\, t > T$.
For $\forall\, t > T$, we have

$$\begin{aligned}
\frac{dy}{dt} &= \{r(1-y) - \eta x\}y \\
&\le \{r - \eta(\underline{x} - \epsilon)\}y \\
&= -\eta\left[\underline{x} - \epsilon - \frac{r}{\eta}\right]y \\
&= -\mu\eta y, \ \left[\text{where } \mu = \underline{x} - \epsilon - \frac{r}{\eta} > 0\right]
\end{aligned}$$

Hence, $\lim_{t\to\infty} y = 0$. □

Remark 4.6. *If the anti-predation rate exceeds the growth rate of the predator and hunts juvenile predator frequently, then the predator population goes extinct from the system as time goes.*

4.2. Considering Specialist predator:

Here we use the facts that $\overline{x} \leq 1$ and $\overline{y} \leq M$ (as the solutions are bounded).
First two theorems give the extinction criterion of prey species and the last two provide the criterion for predator extinction.

Theorem 4.7. *If* $\overline{x} < p$, *then* $\lim_{t\to\infty} x = 0$.

Theorem 4.8. *If* $m\underline{y} > (p+2)(1+a)$, *then* $\lim_{t\to\infty} x = 0$.

Proofs of the above stated theorems are same as the proofs of Theorem 4.1 and Theorem 4.3.

Theorem 4.9. *If* $2cm_1 < d$, *then* $\lim_{t\to\infty} y(t) = 0$.

Proof. Choose ϵ such that for $0 < \epsilon < 1$, $\exists\ T > 0$, s.t. $x(t) < 1 + \epsilon,\ \forall\, t > T$.
For $\forall\, t > T$, we have

$$\begin{aligned}\frac{dy}{dt} = \left\{\frac{cm_1x}{1+ax} - d - \eta x\right\} y &\leq \left\{\frac{cm_1x}{1+ax} - d\right\} y \\ &\leq [cm_1(1+\epsilon) - d]\, y \\ &\leq [2cm_1 - d]\, y \\ &= -\mu y, \ \ [\text{where } \mu = d - 2cm_1 > 0]\end{aligned}$$

Hence, $\lim_{t\to\infty} y = 0$. □

Remark 4.10. *If the mortality rate of predator exceeds its growth rate after consumption of prey, then the predator population goes extinct from the system with time.*

Theorem 4.11. *If* $\eta\underline{x} > cm_1$, *then* $\lim_{t\to\infty} y(t) = 0$.

Proof. Choose ϵ such that for $0 < \epsilon < \underline{x} - \frac{cm}{\eta}$, $\exists\ T > 0$, s.t. $x(t) > \underline{x} - \epsilon,\ \forall\, t > T$.
For $\forall\, t > T$, we have

$$\begin{aligned}\frac{dy}{dt} &= \left\{\frac{cm_1x}{1+ax} - d - \eta x\right\} y \\ &\leq \{cm_1 - \eta(\underline{x} - \epsilon)\} y \\ &= -\eta\left[\underline{x} - \epsilon - \frac{cm_1}{\eta}\right] y \\ &= -\mu\eta y, \ \ \left[\text{where } \mu = \underline{x} - \epsilon - \frac{cm_1}{\eta} > 0\right]\end{aligned}$$

Hence, $\lim_{t\to\infty} y = 0$. □

Remark 4.12. *If the anti-predation rate of predator grows higher than the biomass conversion rate, then predator species cannot sustain in the system in the long run.*

5. Equilibrium Points

The proposed system (2.2) has the following equilibrium points:

1. Trivial Equilibrium Point: $E_0(0,0)$.
2. Axial Equilibrium Points: (i) $E_1(p,0)$, (ii) $E_2(1,0)$ and (iii) $E_3(0,1)$.
3. Interior Equilibrium Point $E^*(x^*,y^*)$ where $y^* = \frac{r-\eta x^*}{r}$ and x^* is the positive root of the equation:

$$G(x) \equiv C_1x^3 + C_2x^2 + C_3x + C_4 = 0, \tag{5.1}$$

where, $C_1 = ar > 0$,
$C_2 = r\{1-a(1+p)\}$,
$C_3 = r(ap-p-1) - m\eta$,
$C_4 = r(p+m) > 0$

For E^*, y^* exists only when $\eta x^* < r$.
Equation (5.1) has no real roots if $1-a(1+p) > 0$ and $r(ap-p-1) > m\eta$ hold. Also, equation (5.1) has either no real roots or two real roots if
(a) $1-a(1+p) < 0$ and $r(ap-p-1) < m\eta$;
(b) $1-a(1+p) > 0$ and $r(ap-p-1) < m\eta$;
(c) $1-a(1+p) < 0$ and $r(ap-p-1) > m\eta$.

Further system (2.4) has the following equilibrium points:

1. Trivial Equilibrium Point: $E_0(0,0)$.
2. Axial Equilibrium Points: (i) $E_1(p,0)$, (ii) $E_2(1,0)$.
3. Interior Equilibrium Point $E^*(x^*,y^*)$ where $y^* = \frac{1}{m}(1+ax^*)(1-x^*)(x^*-p)$ and x^* is the positive root of the equation:

$$G_1(x) = K_1x^2 + K_2x + K_3 = 0, \tag{5.2}$$

where, $K_1 = a\eta > 0$,
$K_2 = \eta + ad - cm_1$,
$K_3 = d > 0$

Equation (5.2) has no real roots if $\eta + ad > cm_1$. Also, it has either no real roots or two real roots if $\eta + ad < cm_1$ holds. Specifically, we get two interior equilibrium points (x_i^*, y_i^*) for $i = 1,2$ if $\eta + ad < cm_1$ holds along with $K_2^2 > 4K_1K_3$. Moreover when $(\eta + ad - cm_1)^2 = 4ad\eta$, two interior equilibrium points coincide each other resulting in a single interior equilibrium point $E^*(x^*,y^*)$.

6. Local Stability Analysis

Local stability conditions of the equilibrium points can be determined by the eigenvalues of corresponding Jacobian matrices. According to the Routh-Hurwitz criterion, an equilibrium point is locally asymptotically stable (LAS) if the Jacobian matrix of the corresponding equilibrium point has all eigenvalues with negative real parts and unstable if one eigenvalue becomes positive. Now, we analyse the Jacobian matrix for each of the equilibrium point for both systems (2.2) and (2.4) one by one to study whether an equilibrium point is stable.

6.1. Generalist predator

Now, the Jacobian matrix of system (2.2) is given by

$$J = \begin{pmatrix} a_{11} & a_{12} \\ a_{21} & a_{22} \end{pmatrix}$$

where $a_{11} = (1-x)(x-p) - x(2x-p-1) - \frac{my}{(1+ax)^2}$; $a_{12} = -\frac{mx}{1+ax}$; $a_{21} = -\eta y$; $a_{22} = r(1-2y) - \eta x$.

$$\text{For } E_0 = (0,0): \ J|_{E_0} = \begin{pmatrix} -p & 0 \\ 0 & r \end{pmatrix}.$$

So, $\lambda_1 = -p < 0$ and $\lambda_2 = r > 0$. So, we have the following theorem:

Theorem 6.1. *E_0 is always a saddle point.*

$$\text{For } E_1 = (p,0): \ J|_{E_1} = \begin{pmatrix} p(1-p) & -\frac{mp}{1+ap} \\ 0 & r - p\eta \end{pmatrix}.$$

So, $\lambda_1 = p(1-p) > 0$ and $\lambda_2 = r - p\eta$. So, we have the following theorem:

Theorem 6.2. *E_1 is saddle point when $r < p\eta$ and unstable when $r > p\eta$.*

$$\text{For } E_2 = (1,0): \ J|_{E_2} = \begin{pmatrix} -(1-p) & -\frac{m}{1+a} \\ 0 & r - \eta \end{pmatrix},$$

So, the eigenvalues are $\lambda_1 = -(1-p) < 0$ and $\lambda_2 = r - \eta$.

Theorem 6.3. *E_2 is stable point when $r < \eta$ and saddle when $r > \eta$.*

$$\text{For } E_3 = (0,1): \ J|_{E_3} = \begin{pmatrix} -(m+p) & 0 \\ -\eta & -r \end{pmatrix},$$

Here, the eigenvalues are $\lambda_1 = -(m+p) < 0$ and $\lambda_2 = -r < 0$. So, we have the following theorem:

Theorem 6.4. *E_3 is always a stable equilibrium point.*

$$\text{Now, for } E^*(x^*, y^*): \ J|_{E^*} = \begin{pmatrix} a_{11} & a_{12} \\ a_{21} & a_{22} \end{pmatrix},$$

where $a_{11} = \dfrac{max^*y^*}{(1+ax^*)^2} - x^*(2x^* - p - 1)$, $a_{12} = -\dfrac{mx^*}{1+ax^*}$, $a_{21} = -\eta y^*$, $a_{22} = -ry^*$.
Characteristic equation for $E^*(x^*, y^*)$ will be

$$\lambda^2 + P_1\lambda + P_2 = 0, \tag{6.1}$$

where $P_1 = -(a_{11} + a_{22})$ and $P_2 = a_{11}a_{22} - a_{12}a_{21}$.
By Routh-Hurwitz criterion all the roots of equation (6.1) have negative real parts if $P_1 > 0$ and $P_2 > 0$. Now $P_2 > 0$ when $a_{11} < 0$. Hence, we have the following theorem:

Theorem 6.5. *$E^*(x^*, y^*)$ will be LAS by Routh-Hurwitz criterion if $a_{11} < 0$, i.e., $max^*y^* < x^*(2x^* - p - 1)(1 + ax^*)^2$.*

6.2. Specialist predator

Now, the Jacobian matrix of system (2.4) is given by

$$J = \begin{pmatrix} a_{11} & a_{12} \\ a_{21} & a_{22} \end{pmatrix}$$

where $a_{11} = (1-x)(x-p) - x(2x-p-1) - \dfrac{m_1 y}{(1+ax)^2}$; $a_{12} = -\dfrac{m_1 x}{1+ax}$; $a_{21} = \dfrac{cm_1 y}{(1+ax)^2} - \eta y$; $a_{22} = \dfrac{cm_1 x}{1+ax} - d - \eta x$.

$$\text{For } E_0 = (0,0): \ J|_{E_0} = \begin{pmatrix} -p & 0 \\ 0 & -d \end{pmatrix}.$$

So, $\lambda_1 = -p < 0$ and $\lambda_2 = -d < 0$. So, we have the following theorem:

Theorem 6.6. *E_0 is always a stable point.*

$$\text{For } E_1 = (p,0): \ J|_{E_1} = \begin{pmatrix} p(1-p) & -\frac{mp}{1+ap} \\ 0 & \frac{cm_1 p}{1+ap} - d - \eta p \end{pmatrix}.$$

So, $\lambda_1 = p(1-p) > 0$ and $\lambda_2 = \dfrac{cm_1 p}{1+ap} - d - \eta p$. So, we have the following theorem:

Theorem 6.7. *E_1 is saddle point when $cm_1 p < (d+\eta p)(1+ap)$ and unstable when $cm_1 p > (d+\eta p)(1+ap)$.*

$$\text{For } E_2 = (1,0): \ J|_{E_2} = \begin{pmatrix} -(1-p) & -\frac{m_1}{1+a} \\ 0 & \frac{cm_1}{1+a} - d - \eta \end{pmatrix},$$

So, the eigenvalues are $\lambda_1 = -(1-p) < 0$ and $\lambda_2 = \dfrac{cm_1}{1+a} - d - \eta$.

Theorem 6.8. *E_2 is stable point when $cm_1 < (d+\eta)(1+a)$ and saddle when $cm_1 > (d+\eta)(1+a)$.*

$$\text{Now, for } E^*(x^*, y^*): \ J|_{E^*} = \begin{pmatrix} a_{11} & a_{12} \\ a_{21} & a_{22} \end{pmatrix},$$

where $a_{11} = \dfrac{m_1 a x^* y^*}{(1+ax^*)^2} - x^*(2x^* - p - 1)$, $a_{12} = -\dfrac{m_1 x^*}{1+ax^*}$, $a_{21} = \left\{ \dfrac{cm_1}{(1+ax^*)^2} - \eta \right\} y^*$, $a_{22} = 0$.
Characteristic equation for $E^*(x^*, y^*)$ will be

$$\lambda^2 + Q_1 \lambda + Q_2 = 0, \tag{6.2}$$

where $Q_1 = -a_{11}$ and $Q_2 = -a_{12}a_{21}$.
By Routh-Hurwitz criterion all the roots of equation (6.2) have negative real parts if $Q_1 > 0$ and $Q_2 > 0$. Now $Q_1 > 0$ when $a_{11} < 0$ and $Q_2 > 0 \Rightarrow cm_1 > \eta(1+ax^*)^2$. Hence, we have the following theorem:

Theorem 6.9. *$E^*(x^*, y^*)$ will be LAS by Routh-Hurwitz criterion if $m_1 a x^* y^* < x^*(2x^* - p - 1)(1+ax^*)^2$ along with $cm_1 > \eta(1+ax^*)^2$.*

7. Bifurcation Analysis

Change of stability around the equilibria have been discussed in this section. We have used **Sotomayor's Theorem** [24] and the Hopf Bifurcation Theorem [21] to observe the bifurcation analysis of both system (2.2) and system (2.4). In order to apply Sotomayor's Theorem, the Jacobian matrix at the bifurcating equilibrium point contains one zero eigenvalue.
Let $V = (v_1, v_2)^T$ and $W = (w_1, w_2)^T$ be the eigenvectors of $J|_{(eq.\ point)}$ and $J|^T_{(eq.\ point)}$ respectively corresponding to zero eigenvalue of the equilibrium point.
Let $F = (F_1, F_2)^T$ and $H = (H_1, H_2)^T$ where
$F_1 = x(1-x)(x-p) - \dfrac{mxy}{1+ax}$,
$F_2 = ry(1-y) - \eta xy$;
$H_1 = x(1-x)(x-p) - \dfrac{m_1xy}{1+ax}$,
$H_2 = \dfrac{m_1xy}{1+ax} - dy - \eta xy$.

Theorem 7.1. *System (2.2) undergoes a transcritical bifurcation with respect to the bifurcation parameter η around $E_2(1,0)$ if $\eta = r$.*

Proof.

$$J|_{E_2} = \begin{pmatrix} p-1 & -\frac{m}{1+a} \\ 0 & r-\eta \end{pmatrix}$$

Let, $\eta_{[TC_1]}$ be the value of η such that $J|_{E_2}$ has a simple zero eigenvalue at $\eta = \eta_{[TC_1]}$.
So, at $\eta = \eta_{[TC_1]}$:

$$J|_{E_2} = \begin{pmatrix} p-1 & -\frac{m}{1+a} \\ 0 & 0 \end{pmatrix}.$$

Here, $\lambda_1 = p - 1 < 0$.
After some calculations: $V = (m, (p-1)(1+a))^T$ and $W = (0,1)^T$.

$$\begin{aligned} \text{So, } \Omega_1 &= W^T.F_\eta(E_2, \eta_{[TC_1]}) = -xy|_{E_2} = 0, \\ \Omega_2 &= W^T\left[DF_\eta(E_2, \eta_{[TC_1]})V\right] = -xv_2|_{E_2} = (1-p)(1+a) \neq 0 \\ \text{and } \Omega_3 &= W^T\left[D^2F(E_2, \eta_{[TC_1]})(V,V)\right] = 2(1-p)(1+a)[m\eta + r(p-1)(1+a)] \neq 0. \end{aligned}$$

By Sotomayor's Theorem, system (2.2) undergoes a transcritical bifurcation around E_2 at $\eta = \eta_{[TC_1]}$. □

Theorem 7.2. *System (2.2) undergoes a saddle-node bifurcation with respect to the bifurcation parameter p around $E^*(x^*, y^*)$ when $G(x) = 0$ has a double root in the interval $(p, 1)$.*

Proof. Let $x_{[sn_1]}$ be a double root of $G(x) = 0$ such that $p < x_{[sn_1]} < 1$. So, $G(x_{[sn_1]}) = 0 = G'(x_{[sn_1]})$ and $G''(x_{[sn_1]}) \neq 0$. Let $p_{[sn_1]}$ be the threshold value of p such that for $p = p_{[sn_1]}$, $x_{[sn_1]}$ is a double root of $G(x) = 0$. The non-trivial nullclines touch each other at $(x_{[sn_1]}, p_{[sn_1]}) \equiv E^*_{[sn_1]}$. Let, $F_1(x,y) = xf_1(x,y)$, $F_2(x,y) = yf_2(x,y)$. $\left.\frac{dy^{(f_1)}}{dx}\right|_{E^*_{[sn_1]}}$ denote slope of $f_1(x,y) = 0$ and $\left.\frac{dy^{(f_2)}}{dx}\right|_{E^*_{[sn_1]}}$ denote slope of $f_2(x,y) = 0$. Now, $\left.\frac{dy^{(f_1)}}{dx}\right|_{E^*_{[sn_1]}} = -\left.\frac{\partial F_1/\partial x}{\partial F_1/\partial y}\right|_{E^*_{[sn_1]}}$, $\left.\frac{dy^{(f_2)}}{dx}\right|_{E^*_{[sn_1]}} = -\left.\frac{\partial F_2/\partial x}{\partial F_2/\partial y}\right|_{E^*_{[sn_1]}}$.

$$J|_{E^*} = \begin{pmatrix} \frac{\partial F_1}{\partial x} & \frac{\partial F_1}{\partial y} \\ \frac{\partial F_2}{\partial x} & \frac{\partial F_2}{\partial y} \end{pmatrix} = \begin{pmatrix} x\frac{df_1}{dx} & x\frac{df_1}{dy} \\ y\frac{df_2}{dx} & y\frac{df_2}{dy} \end{pmatrix} = \begin{pmatrix} a_{11} & a_{12} \\ a_{21} & a_{22} \end{pmatrix}$$

where $a_{11} = \frac{max^*y^*}{(1+ax^*)^2}$, $a_{12} = -\frac{mx^*}{1+ax^*}$, $a_{21} = -\eta y^*$, $a_{22} = -ry^*$.
Here, $Det\left(J|_{E^*_{[sn_1]}}\right) = xy\left[\frac{df_1}{dx}\frac{df_2}{dy} - \frac{df_1}{dy}\frac{df_2}{dx}\right] = 0$ as $\frac{dy^{(f_1)}}{dx}\Big|_{E^*_{[sn_1]}} = \frac{dy^{(f_2)}}{dx}\Big|_{E^*_{[sn_1]}}$. Thus the Jacobian matrix $J|_{E^*_{[sn_1]}}$ has a simple zero eigenvalue.
Here, $V = (a_{22}, -a_{21})^T$ and $W = (a_{22}, -a_{12})^T$.

$$\text{so, } \Omega_1 = W^T.F_p(E^*, p_{[sn_1]}) = -a_{22}x^*(1-x^*)\Big|_{E^*_{[sn_1]}} \neq 0$$

$$\text{and } \Omega_2 = W^T\left[D^2F(E^*, p_{[sn_1]})(V,V)\right] = [a_{22}(2f_{1xy}v_2 + f_{1xx}v_1)v_1 + 2a_{12}v_2(v_1\eta + rv_2)]\Big|_{E^*_{[sn_1]}} \neq 0.$$

Thus, from Sotomayor's Theorem, system (2.2) undergoes a non-degenerate saddle-node bifurcation around E^* at $p = p_{[sn_1]}$. □

- **Non-occurrence of Hopf bifurcation:**
  Characteristic equation of $E^* : \lambda^2 + P_1\lambda + P_2 = 0$.
  Here $P_1 = -(a_{11} + a_{22})$ and $P_2 = a_{11}a_{22} - a_{12}a_{21}$ where $a_{11} = \frac{max^*y^*}{(1+ax^*)^2}$, $a_{12} = -\frac{mx^*}{1+ax^*}$, $a_{21} = -\eta x^*$, $a_{22} = -ry^*$.
  Hopf bifurcation around E^* occurs when $Tr(J|_{E^*}) = P_1 = 0$ with $Det(J|_{E^*}) = P_2 > 0$. Now, $P_1 = 0$ implies $a_{11} = -a_{22}$ and this gives $P_2 = -a_{22}^2 - a_{12}a_{21} < 0$. As we get $Det(J|_{E^*})$ as negative, hence, Hopf bifurcation can not occur around E^* for any parameter values.

A co-dimensional 2 bifurcation is cusp bifurcation where the critical equilibrium point has a zero eigenvalue and the quadratic coefficient for the saddle-node bifurcation vanishes. Two branches of saddle-node bifurcation curve or a saddle-node bifurcation curve and one transcritical bifurcation curve meet tangentially at the cusp bifurcation point forming a semicubic parabola.

Theorem 7.3. *The interior equilibrium point E^* of system (2.2) undergoes cusp bifurcation at the threshold $(p, \eta) = (p_{[CP]}, \eta_{[CP]})$ around $E^*(x^*, y^*)$ when $G(x) = 0$ in equation (5.1) has a triple root in Ω_1 (which stated in Theorem 3.2).*

Proof. Let x_3 be a triple root of $G(x) = 0$, $G(x_3) = G'(x_3) = G''(x_3) = 0$ and $G'''(x_3) \neq 0$. Now proceeding as Theorem 8.2, it can be shown that the Jacobian matrix at $E^*_{[CP]}(x_3, y_3)$ $\left(\text{denoted by, } J|_{E^*_{[CP]}}\right)$ has one zero eigenvalue. Moreover, the quadratic normal form coefficient for the saddle-node bifurcation at $E^*_{[CP]}$ is given by

$$W^T\left[D^2F(E^*_{[CP]}, p_{[CP]})(V,V)\right] = 0.$$

Hence system (2.2) undergoes a co-dimension two bifurcation which is known as cusp bifurcation at $(p, \eta) \equiv (p_{[CP]}, \eta_{[CP]})$ and the point $(p_{[CP]}, \eta_{[CP]})$ in the p-η parametric plane is the intersection of the two branches of saddle-node bifurcation, where they meet each other tangentially. □

Theorem 7.4. *System (2.4) undergoes a transcritical bifurcation with respect to the bifurcation parameter η around $E_2(1, 0)$ if $cm_1 = (d + \eta)(1 + a)$.*

Proof.

$$J|_{E_2} = \begin{pmatrix} p-1 & -\frac{m}{1+a} \\ 0 & \frac{cm_1}{1+a} - d - \eta \end{pmatrix}$$

Let, $\eta_{[TC_2]}$ be the value of η such that $J|_{E_2}$ has a simple zero eigenvalue at $\eta = \eta_{[TC_2]}$.
So, at $\eta = \eta_{[TC_2]}$:

$$J|_{E_2} = \begin{pmatrix} p-1 & -\frac{m}{1+a} \\ 0 & 0 \end{pmatrix}.$$

Here, $\lambda_1 = p - 1 < 0$.
After some calculations: $V = (m_1, (p-1)(1+a))^T$ and $W = (0,1)^T$.

$$\text{So, } \Omega_1 = W^T.H_\eta(E_2, \eta_{[TC_2]}) = -xy|_{E_2} = 0,$$
$$\Omega_2 = W^T\left[DH_\eta(E_2, \eta_{[TC_2]})V\right] = -xv_2|_{E_2} = (1-p)(1+a) \neq 0$$
$$\text{and } \Omega_3 = W^T\left[D^2H(E_2, \eta_{[TC_2]})(V,V)\right] = \frac{2m_1(p-1)}{1+a}\{d(1+a)^2 - acm_1\} \neq 0.$$

By Sotomayor's Theorem, system (2.4) undergoes a transcritical bifurcation around E_2 at $\eta = \eta_{[TC_2]}$. □

Theorem 7.5. *System (2.4) undergoes a saddle-node bifurcation with respect to the bifurcation parameter η around $E^*(x^*, y^*)$ when $(\eta + ad - cm_1)^2 = 4ad\eta$.*

Proof.

$$J|_{E^*} = \begin{pmatrix} a_{11} & a_{12} \\ a_{21} & 0 \end{pmatrix}$$

where $a_{11} = \frac{m_1 a x^* y^*}{(1+ax^*)^2} - x^*(2x^* - p - 1)$, $a_{12} = -\frac{m_1 x^*}{1+ax^*}$, $a_{21} = \left\{\frac{cm_1}{(1+ax^*)^2} - \eta\right\} y^*$.
Characteristic equation for $E^*(x^*, y^*)$ will be $\lambda^2 - a_{11}\lambda + Q_2 = 0$ where $Q_2 = -a_{12}a_{21} = -\frac{m_1 x^* y^*}{(1+ax^*)}\left\{\frac{cm_1}{(1+ax^*)^2} - \eta\right\}$.
At $\eta = \eta_{[sn_2]}$, we have $(\eta + ad - cm_1)^2 = 4ad\eta$, i.e., $cm_1 = \eta(1+ax^*)^2$ resulting in $Q_2 = 0$. Thus the Jacobian matrix $J|_{E^*_{[sn_2]}}$ has a simple zero eigenvalue. So, at $\eta = \eta_{[sn_2]}$:

$$J|_{E^*} = \begin{pmatrix} a_{11} & a_{12} \\ 0 & 0 \end{pmatrix},$$

where, $\lambda_1 = a_{11} < 0$ (by one of the stability condition of E^*).
The calculations give: $V = (a_{12}, -a_{11})^T$ and $W = (0,1)^T$.

$$\text{so, } \Omega_1 = W^T.H_\eta(E^*, \eta_{[sn_2]}) = -xy\Big|_{E^*_{[sn_2]}} \neq 0$$
$$\text{and } \Omega_2 = W^T\left[D^2H(E^*, \eta_{[sn_2]})(V,V)\right] = -\frac{2acm_1y^*}{(1+ax^*)^2}v_1^2 \neq 0.$$

Thus, from Sotomayor's Theorem, system (2.4) undergoes a non-degenerate saddle-node bifurcation around E^* at $\eta = \eta_{[sn_2]}$. □

Hopf Bifurcation at $E^*(x^*, y^*)$:
Let us consider η as bifurcation parameter to check the instability of the equilibrium point E^*. The characteristic equation of system (2.4) at $E^*(x^*, y^*)$ is

$$\lambda^2 + Q_1\lambda + Q_2 = 0, \tag{7.1}$$

$$\text{where, } Q_1 = -a_{11} = -\left[\frac{m_1 a x^* y^*}{(1+ax^*)^2} - x^*(2x^* - p - 1)\right],$$
$$Q_2 = -a_{12}a_{21} = \frac{m_1 x^* y^*}{1+ax^*}\left\{\frac{cm_1}{(1+ax^*)^2} - \eta\right\}$$

Theorem 7.6. *If E^* exists with the feasibility conditions, then a simple Hopf bifurcation occurs at unique $\eta = \eta_0$, where η_0 is the unique positive root of the equation: $Q_1(\eta) = 0$ with $Q_2(\eta_0) > 0$.*

Proof. For $\eta = \eta_0$, the characteristic equation of system (2.4) at E^* is $\lambda^2 + Q_2 = 0$
which gives roots: $\lambda_1 = i\sqrt{Q_2}$ and $\lambda_2 = -i\sqrt{Q_2}$. So there exists a pair of purely imaginary eigenvalues. Also, $Q_i(\eta)$ are continuous functions of η.
So, for η in a neighbourhood of η_0, the roots have the form:
$\lambda_1 = p_1(\eta) + ip_2(\eta)$, $\lambda_2 = p_1(\eta) - ip_2(\eta)$; $p_i(k)$ are real for $i = 1, 2$.
Next to check the transversality condition: $\frac{d}{d\eta}[Re(\lambda_i(\eta))]|_{\eta=\eta_0} \neq 0$, for $i = 1, 2$.
Put $\lambda(\eta) = p_1(\eta) + ip_2(\eta)$ in (7.1), we get

$$(p_1 + ip_2)^2 + Q_1(p_1 + ip_2) + Q_2 = 0. \tag{7.2}$$

Taking derivative w.r.to k, we get

$$2(p_1 + ip_2)(\dot{p_1} + i\dot{p_2}) + Q_1(\dot{p_1} + i\dot{p_2}) + \dot{Q_1}(p_1 + ip_2) + \dot{Q_2} = 0.$$

Comparing real and imaginary parts:

$$S_1\dot{p_1} - S_2\dot{p_2} + S_3 = 0, \tag{7.3}$$

$$S_2\dot{p_1} + S_1\dot{p_2} + S_4 = 0, \tag{7.4}$$

where $S_1 = 2p_1 + Q_1$; $S_2 = 2p_2$; $S_3 = \dot{Q_1}p_1 + \dot{Q_2}$; $S_4 = \dot{Q_1}p_2$.
From (7.3) and (7.4):

$$\dot{p_1} = -\frac{S_2S_4 + S_1S_3}{S_1^2 + S_2^2}. \tag{7.5}$$

Now,$S_1 = 2p_1 + Q_1 \neq 2p_1$; $S_3 = \dot{Q_1}p_1 + \dot{Q_2} \neq \dot{Q_2}$; $S_4 = \dot{Q_1}p_2 \neq 0$.
At $\eta = \eta_0$:
Case-(1): $p_1 = 0$; $p_2 = \sqrt{Q_2}$.
So, $S_1 \neq 0$; $S_2 = 2\sqrt{Q_2}$; $S_3 \neq \dot{Q_2}$; $S_4 \neq 0$
and $S_2S_4 + S_1S_3 \neq 0$.
Case-(2): $p_1 = 0$; $p_2 = -\sqrt{Q_2}$.
So, $S_1 \neq 0$; $S_2 = -2\sqrt{Q_2}$; $S_3 \neq \dot{Q_2}$; $S_4 \neq 0$
and $S_2S_4 + S_1S_3 \neq 0$.

$$\text{So, } \left(\frac{d}{d\eta}[Re(\lambda_i(\eta))]\right)\Big|_{\eta=\eta_0} = -\frac{S_2S_4 + S_1S_3}{S_1^2 + S_2^2} \neq 0.$$

Hence the theorem. □

In a two parametric plane a local bifurcation of co-dimension two occurs when Hopf-bifurcation curve and saddle-node curve intersect each other and this bifurcation is called Bogdanov-Takens bifurcation.

Theorem 7.7. *The interior equilibrium point E^* of system (2.4) undergoes Bogdanov-Takens bifurcation at the threshold $(\eta, m_1) = (\eta_{[BT]}, m_{1[BT]})$ if $Det(J|_{E^*})|_{(\eta_{[BT]}, m_{1[BT]})} = 0$ and $Tr(J|_{E^*})|_{(\eta_{[BT]}, m_{1[BT]})} = 0$.*

8. Numerical Simulation

Numerical figures play an essential part in any model system because these validate the analytical results. In this work, we have considered a prey-predator system with anti-predator behaviour in presence of both generalist and specialist predator. Let us fix some of the parameters in Table 1.

Parameter	p	m	a	η
Value	0.17	0.5	6	0.6

Table 1: Parametric values used in numerical simulation

Figure 1 depict the nullclines and position of equilibrium points for $r = 1$ and $r = 0.5$. In Figure (1.a), we have taken $r = 0.5$ and got three axial equilibrium points $E_1(p, 0)$, $E_2(1, 0)$, $E_3(0, 1)$ and one interior equilibrium point $E^*(0.32, 0.61)$. But in Figure (1.b), we have taken $r = 1$ and got two interior equilibrium points $E_1^*(0.36, 0.78)$ and $E_2^*(0.96, 0.42)$ along with E_1, E_2 and E_3.

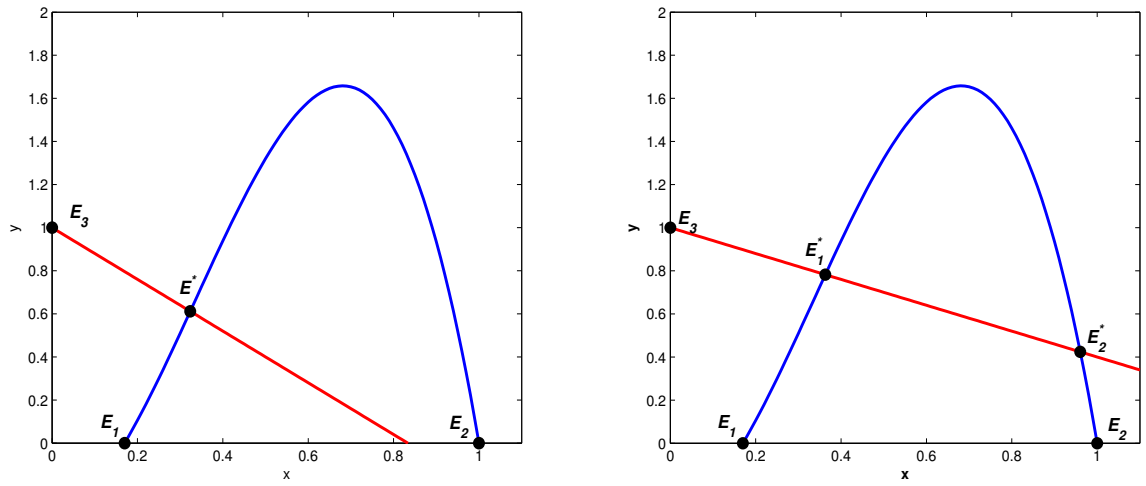

(1.a) *(1.b)*

Figure 1: Position of Prey nullcline ("blue" curve) and Predator nullclines ("red" curve) of system (2.2): (14.a) $r = 0.5$ and (14.b) $r = 1$. Parametric values have been taken from Table 1.

Figure 2 depict that for $r = 1$, the trajectory starting from $x_0 = (0.9, 0.45)$ converges to $E^*(0.96, 0.42)$. Though we get another interior point $(0.36, 0.78)$ but it acts as a saddle point. Again from the same parametric values, if we choose a trajectory with starting point $x_0 = (0.09, 0.45)$, then it tends to prey-free equilibrium $E_3(0, 1)$ (see Figure 3).

So, it is observed that the trajectory can converge to either E_3 or E^* depending on the initial point. A small perturbation in initial point can change the direction of trajectory from interior steady-state to prey-free equilibrium. Hence an occurrence of bistability between E_3 and E^* has been reported (see Figure 4).

Further, Figure 5 show that for $r = 0.5$, trajectory starting from $x_0 = (0.9, 0.045)$ converges to $E_2(1, 0)$. Also, we get one interior point $E^*(0.32, 0.61)$ which is a saddle point. Changing the initial point slightly leads to a trajectory converging towards $E_3(0, 1)$. So, if a trajectory starts from $x_0 = (0.9, 0.45)$, then it approaches towards $(0, 1)$. In this case also, occurrence of bistable behaviour can be observed (see Figure 6).

From the stable state of $E_2(1, 0)$, if the anti-predation rate starts to decrease, then at some threshold value of $\eta = \eta_{[TC]}$, E_2 loses its stability and becomes unstable once η lies below r (intrinsic growth rate of predator species). So, system (2.2) undergoes a transcritical bifurcation around E_2 at $\eta = \eta_{[TC]} = 0.5$ (see Figure 7).

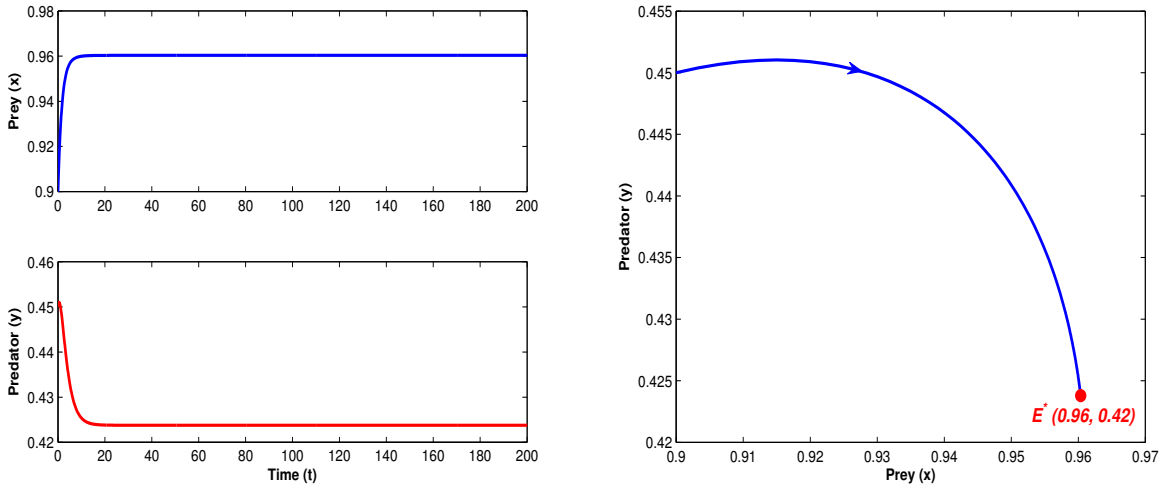

(2.a) (2.b)

Figure 2: Stable behaviour of E^* in system (2.2) for $r = 1$. Parametric values have been taken from Table 1.

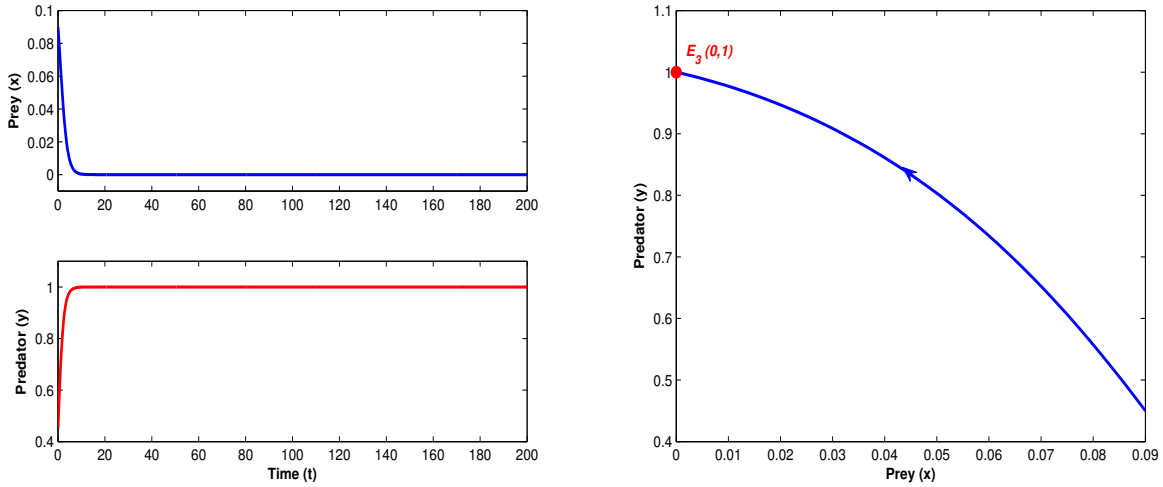

(3.a) (3.b)

Figure 3: Stable behaviour of E_3 in system (2.2) for $r = 1$. Parametric values have been taken from Table 1.

Here Allee threshold (p) plays an important role to control the system dynamics. For $r = 1$, we get a threshold value of $p = p_{[sn]}$, above which there are no equilibrium points but for $p < p_{[sn]}$, there are two equilibrium points among which one is always stable and other one is always unstable. So, at $p = p_{[sn]} = 0.583431$, two equilibria coincide with each other and the system undergoes a saddle-node bifurcation around E^* (see Figure 8) with coordinate $(x_{[sn]}, y_{[sn]}) = (0.837197, 0.497682)$.

Taking (p, η) as bifurcation parameters, we get a co-dimensional 2 bifurcation, named cusp bifurcation. A cusp bifurcation occurs when two saddle-node bifurcation curves or a transcritical curve and a saddle-node bifurcation curve meet tangentially. For $r = 1$, $m = 0.5$ and $a = 6$, the system undergoes a cusp bifurcation (denoted by "CP" in figure 9) with $(p_{[CP]}, \eta_{[CP]}) = (0.928560, 1)$ with coordinate $(0.999996, 0.000004)$. Here the normal form coefficient $c = 7.428197e^{+00}$ which implies the bifurcation is non-degenerate (see Figure 9).

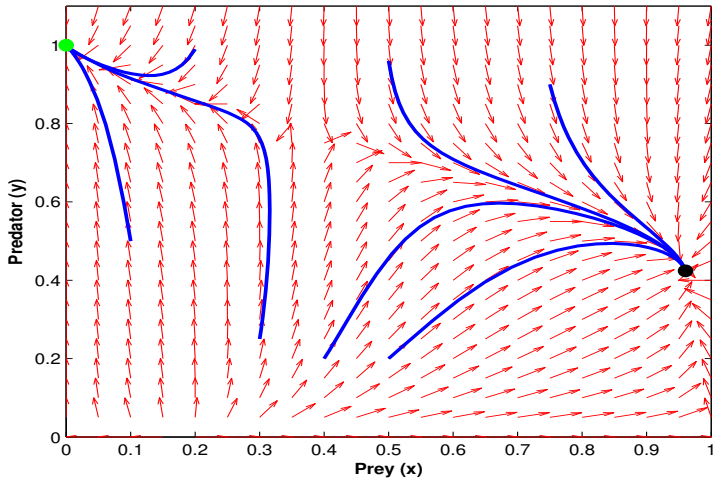

Figure 4: Bistable behaviour between E_3 and E^* of system (2.2) for $r = 1$.. Parametric values have been taken from Table 1.

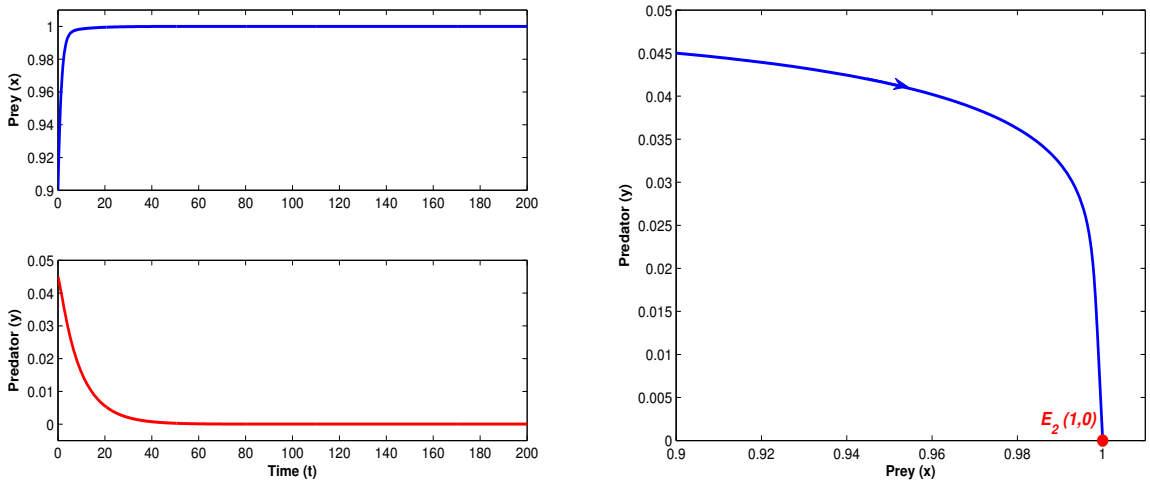

(5.a) *(5.b)*

Figure 5: Stable behaviour of E_2 in system (2.2) for $r = 0.5$. Parametric values have been taken from Table 1.

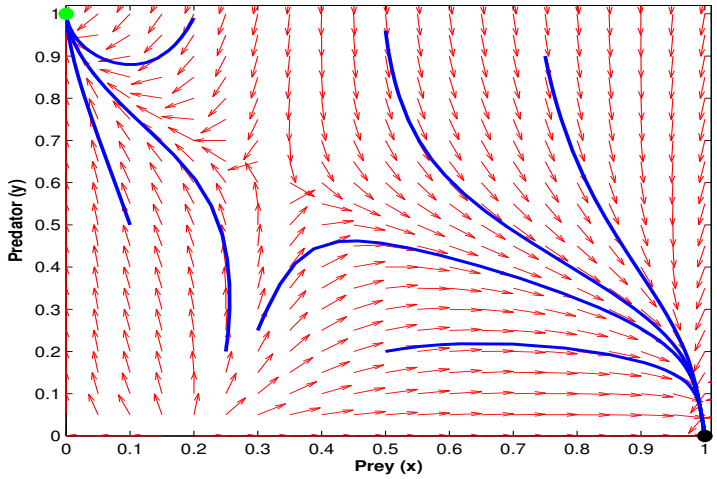

Figure 6: Bistable behaviour between E_2 and E_3 of system (2.2) for $r = 0.5$.. Parametric values have been taken from Table 1.

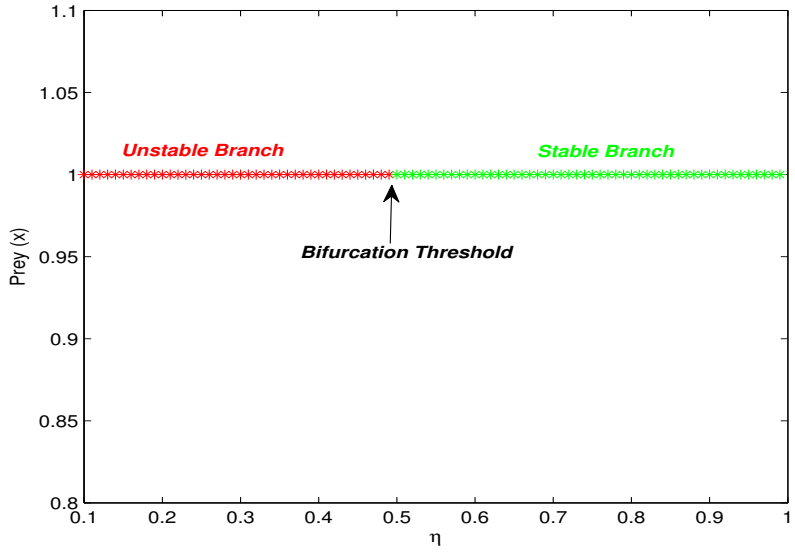

Figure 7: Transcritical Bifurcation around E_2 for $r = 0.5$ in system (2.2) taking η as bifurcation parameter.

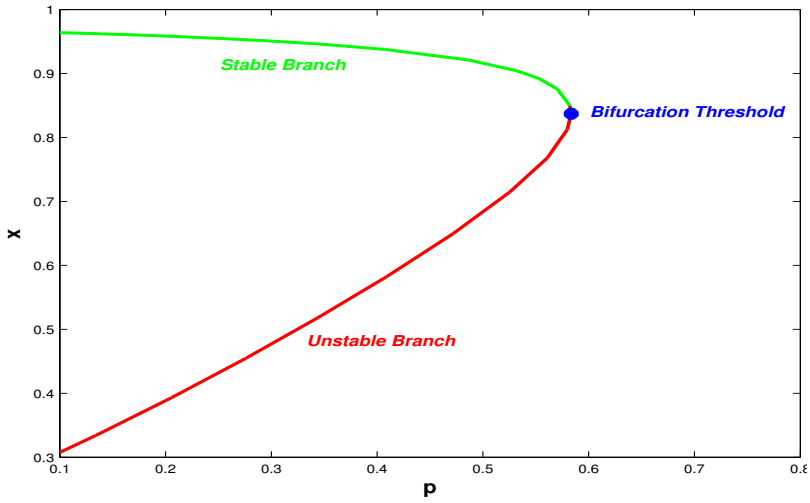

Figure 8: Saddle-node Bifurcation around E^* in system (2.2) for $r = 1$ taking p as bifurcation parameter.

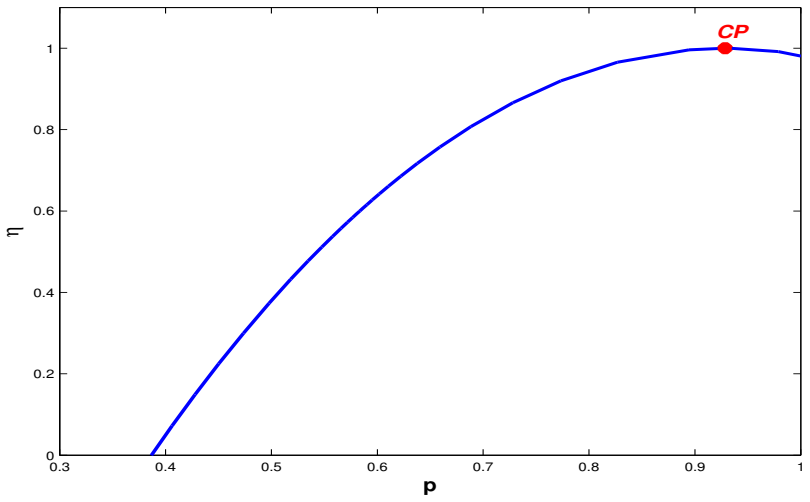

Figure 9: Two parameter bifurcation diagram in system (2.2): Cusp bifurcation in p-η plane where $CP \equiv \left(p_{[CP]},\ \eta_{[CP]}\right)$

Now let us consider another set of parametric values in Table 2. Figure 10 contain the position of

Parameter	p	m	a	r
Value	0.4	0.5	6	1

Table 2: Parametric values used in numerical simulation

nullclines for different values of η. When $\eta = 0.01$, there does not exist any interior equilibrium point (see Figure (10.a)). We get only trivial and axial equilibrium points here. In the next Figure (10.b), the value of η has been slightly increased ($\eta = 0.05$) and we get one interior equilibrium point along with trivial and axial equilibrium points. For increasing value of η, the predator nullcline further moves down and in the next Figure (10.c), i.e., when $\eta = 0.6$, we get two interior equilibrium points E_1^* and E_2^* along with other trivial and axial equilibrium points E_0, E_1, E_2 and E_3. Here, increasing value of η results in non-occurrence of interior point to the occurrence of two interior points.

For $\eta = 0.6$, it is observed in Figure 11 that the trajectory starting from $x_0 = (0.9, 0.45)$ approaches to

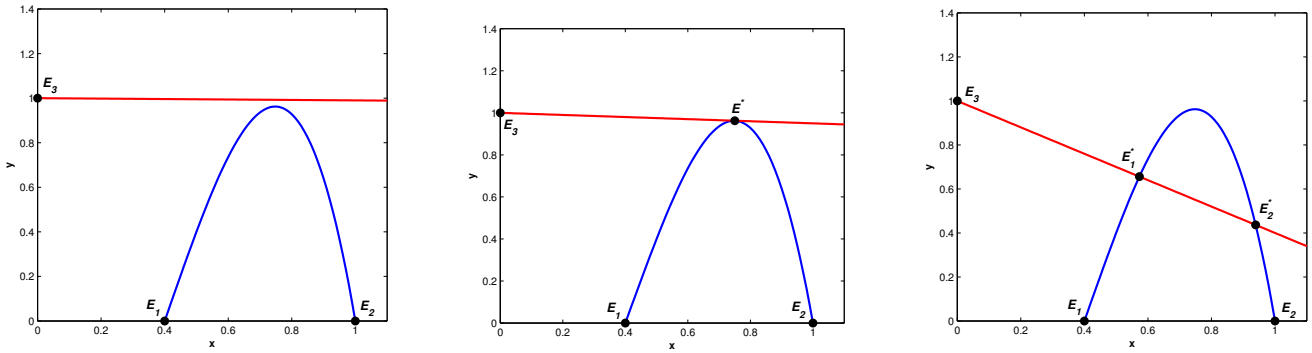

(10.a) *(10.b)* *(10.c)*

Figure 10: Position of Prey nullcline ("blue" curve) and Predator nullclines ("red" curve) of system (2.2): (10.a) $\eta = 0.01$; (10.b) $\eta = 0.05$ and (10.c) $\eta = 0.6$. Parametric values have been taken from Table 2.

$E^*(0.94, 0.44)$. Though there exists another interior $(0.57, 0.66)$, it is a saddle point. Also, $E_3(0, 1)$ is an equilibrium point which is always stable for any parametric values. So, here also we get bistability in the system depending on the choice of initial points. Figure 12 shows that the trajectory if starts from the basin of attraction of E_3, then ultimately converges to E_3 and if any trajectory starts from the basin of attraction of E^*, then it ultimately converges to E^*.

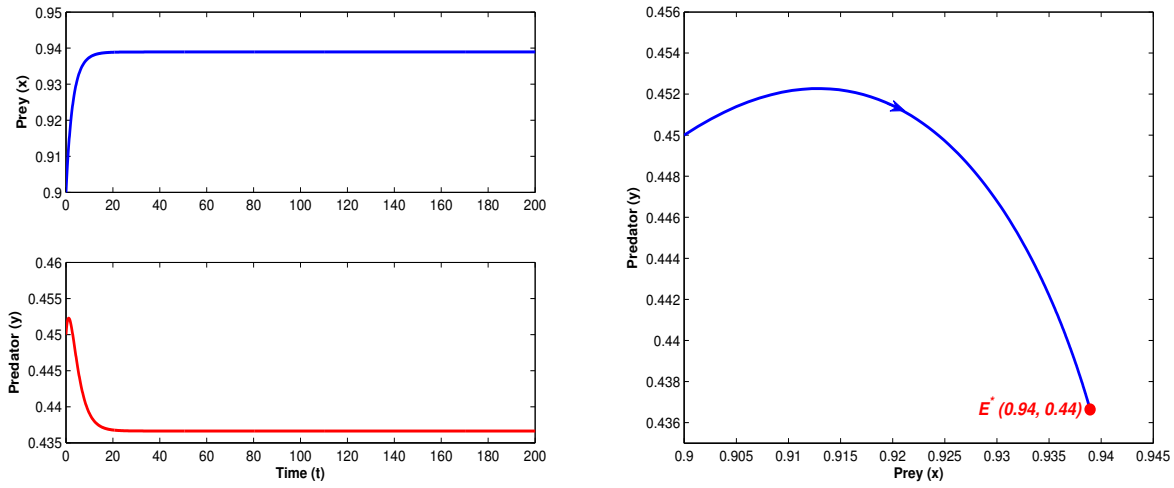

(11.a) (11.b)

Figure 11: Stable behaviour of E^* in system (2.2) for $\eta = 0.6$. Parametric values have been taken from Table 2.

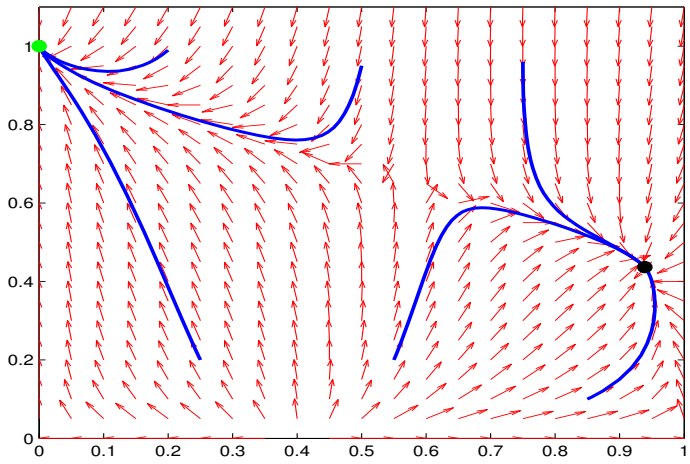

Figure 12: Bistable behaviour between E_3 and E^* of system (2.2) for $\eta = 0.6$.. Parametric values have been taken from Table 2.

Now η plays an important role to control the system dynamics. Figure 13 depicts when η exceeds a threshold value $\eta_{[sn]}$, there are two interior equilibrium points among which one is stable and other one is unstable but when η lies below $\eta_{[sn]}$, there is no interior equilibrium point. So, at $\eta = \eta_{[sn]} = 0.05$, two interior points coincide each other at $E^*(0.75, 0.9625)$ and the system undergoes a saddle-node bifurcation around E^* at $\eta = \eta_{[sn]}$.

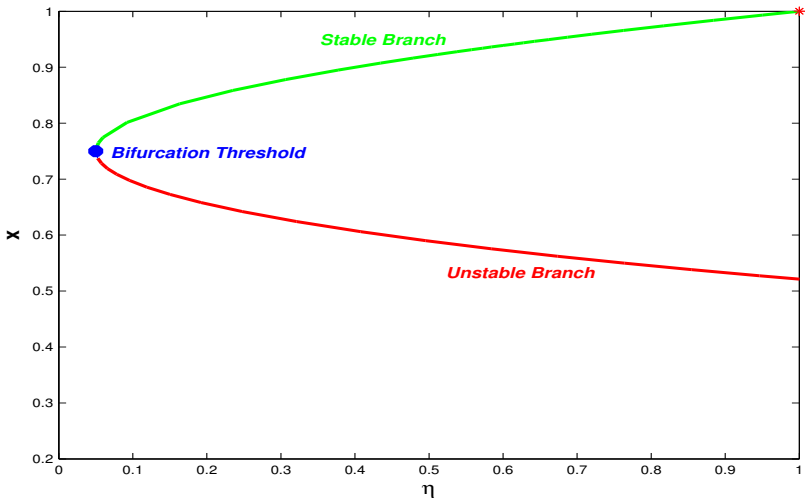

Figure 13: Saddle-node Bifurcation around E^* in system (2.2) taking η as bifurcation parameter. Parameter values have been taken from Table 2.

To observe the impact of anti-predator behaviour in presence of the specialist predator, let us fix some of the parameters in Table 3.

Parameter	p	m_1	a	c	d
Value	0.1	0.3	2	0.4	0.01

Table 3: Parametric values used in numerical simulation

Figure 14 depict the position of nullclines for different values of η along with parametric values in Table 3 in presence of specialist predator. For $\eta = 0.04$, we get the trivial equilibrium point $E_0(0, 0)$, axial equilibrium points $E_1(0.1, 0)$, $E_2(1, 0)$ and two interior equilibrium points $E_1^*(0.25, 0.5625)$ and $E_2^*(0.5, 1.33)$ (see Figure (14.a)). If η starts to decrease, then at $\eta = 0.03$, we get one interior equilibrium point and one of the predator nullclines shift to right in such a way that one of the interior point coincide with $E_2(1, 0)$ (see Figure (14.b)). Further for $\eta = 0.01$, we get only one interior point $E^*(0.11, 0.51)$ along with trivial equilibrium E_0 and axial equilibria E_1, E_2 (see Figure (14.c) and zoomed Figure (14.d)).

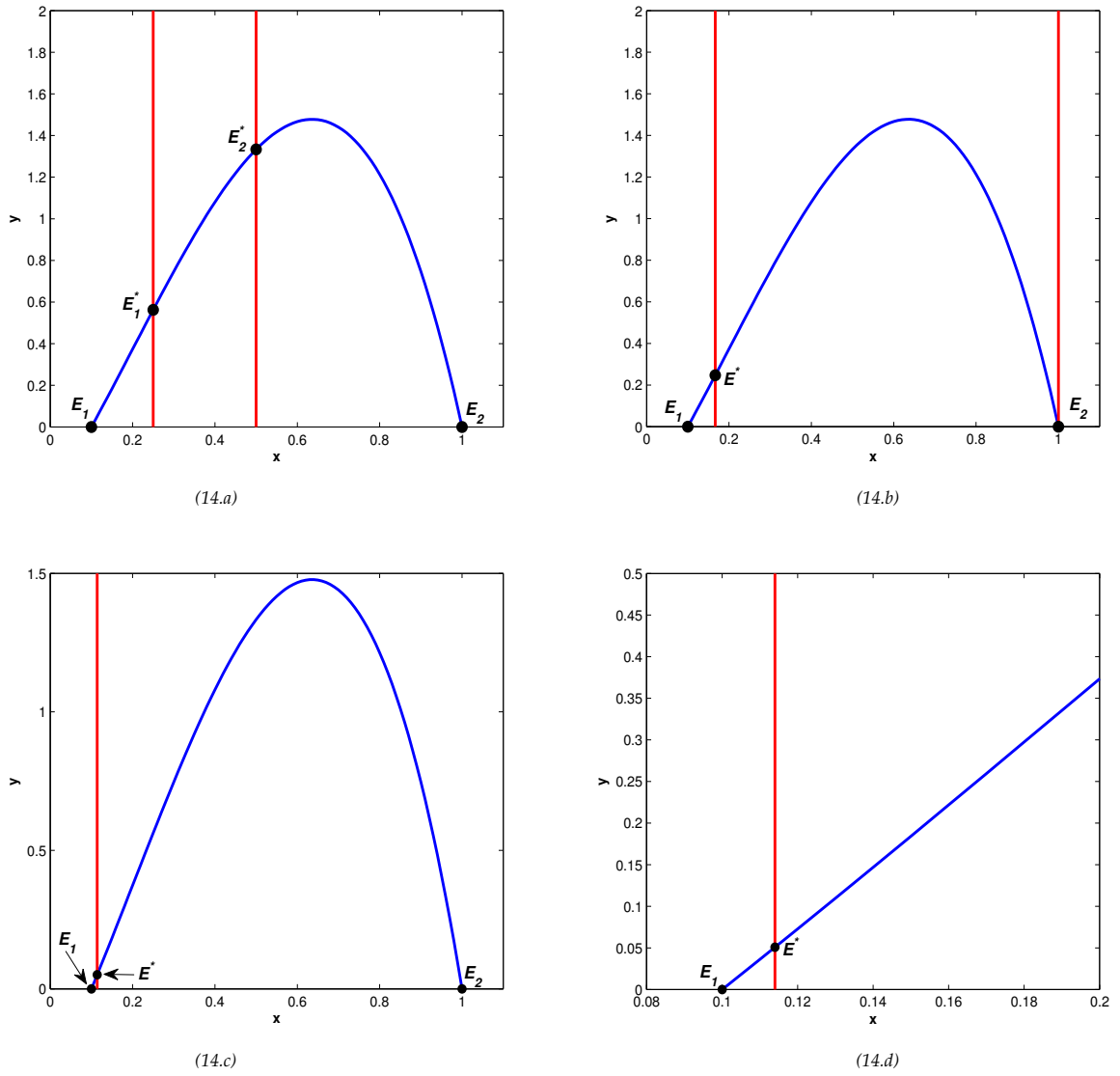

(14.a) (14.b)

(14.c) (14.d)

Figure 14: Position of Prey nullcline ("blue" curve) and Predator nullclines ("red" curve) of system (2.4): (14.a) $\eta = 0.04$; (14.b) $\eta = 0.03$ and (14.c)-(14.d) $\eta = 0.01$. Parametric values have been taken from Table 3.

Next we consider another set of values of the parameters in Table 4 to draw Figures 15–26.

Parameter	p	m_1	a	c	d
Value	0.1	0.3	0.3	0.08	0.002

Table 4: Parametric values used in numerical simulation

Figure 15 shows two positions of nullclines for $\eta = 0.006$ and $\eta = 0.0168$ respectively. Here for the left side figure ($\eta = 0.006$) we get only one feasible interior equilibrium point $E^*(0.12, 0.05)$ along with two axial equilibrium points $E_1(0.1, 0)$ and $E_2(1, 0)$. But in Figure (15.b), we get two interior equilibria $E_1^*(0.48, 0.75)$ and $E_2^*(0.83, 0.51)$ along with E_1 and E_2. Further the calculations give that the interior points for $\eta = 0.017$

be $E_1^*(0.58, 0.79)$ and $E_2^*(0.67, 0.76)$. So, it is observed that for increasing value of η, the distance between two predator nullclines decreases and we get two interior equilibria for a certain range of η.

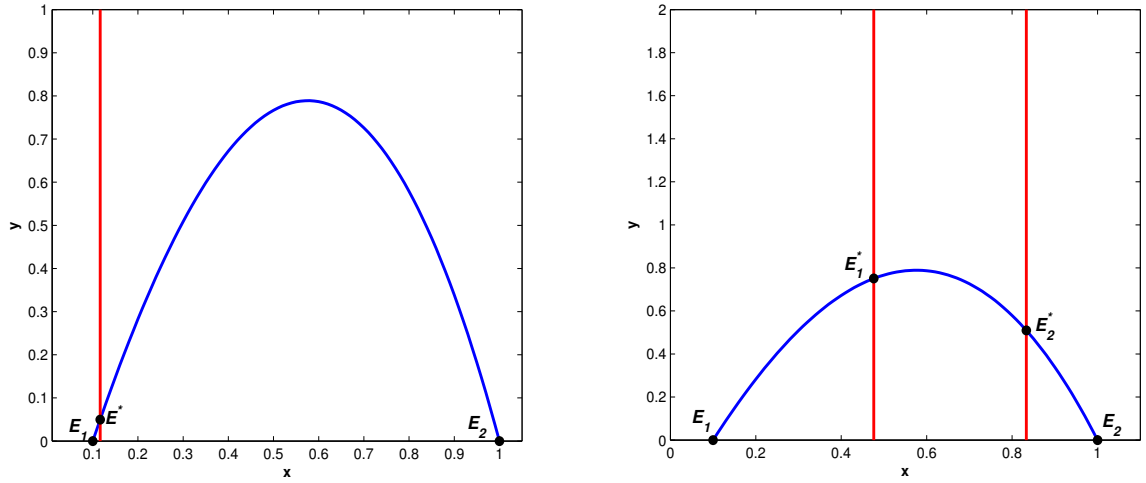

(15.a) (15.b)

Figure 15: Position of Prey nullcline ("blue" curve) and Predator nullclines ("red" curve) of system (2.4): (15.a) $\eta = 0.006$ and (15.b) $\eta = 0.0168$.

In presence of specialist predator, the trivial equilibrium point always acts as a stable equilibrium point due to the strong Allee effect. Taking $\eta = 0.006$, the trajectory starting from $x_0 = (0.5, 0.5)$ approaches to $E_0(0, 0)$ (see Figure 16).

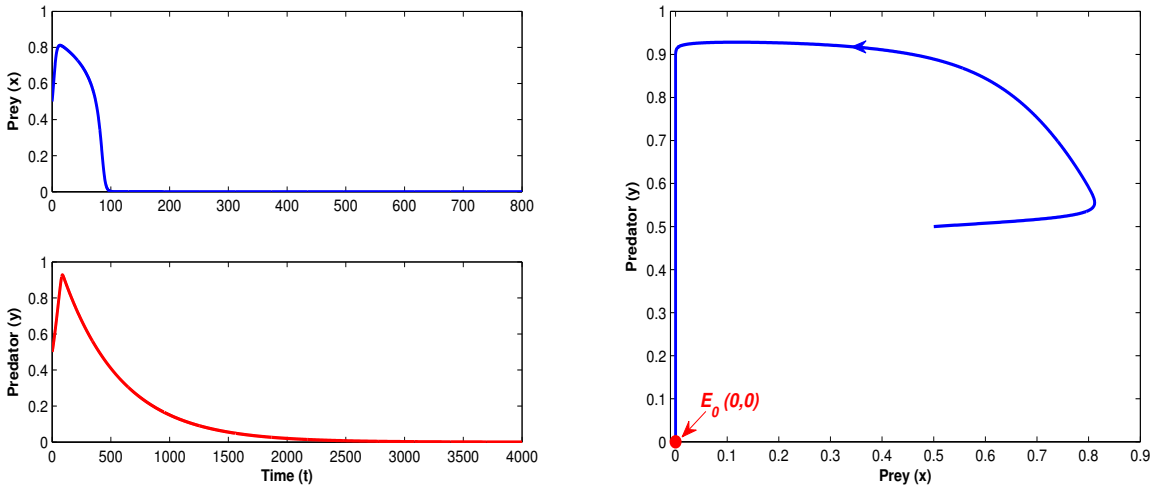

(16.a) (16.b)

Figure 16: Stable behaviour of E_0 in system (2.4) for $\eta = 0.006$.

Further, for an increasing value of η ($\eta = 0.017$), we get a situation where both prey and predator coexists as a steady state. Figure 17 depict that a trajectory starting from $x_0 = (0.55, 0.76)$ converges to the stable

equilibrium point $E^*(0.59, 0.79)$.

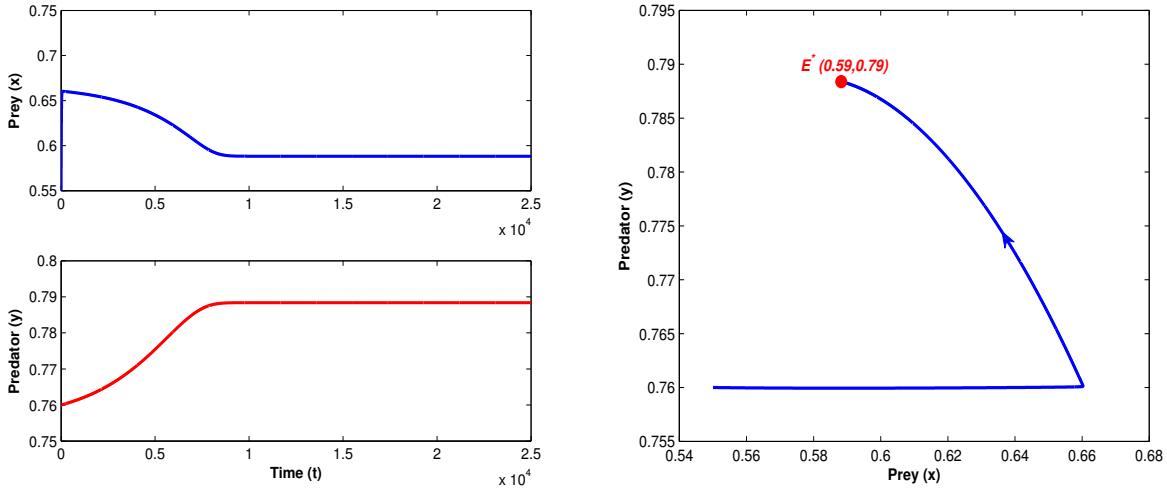

(17.a) *(17.b)*

Figure 17: Stable behaviour of E^* in system (2.4) for $\eta = 0.017$.

Moreover, for $\eta = 0.017$ along with other parameter values stated in Table 4, a trajectory starting from $x_0 = (0.8, 0.05)$ approaches to predator-free equilibrium $E_2(1, 0)$ with time (see Figure 18).

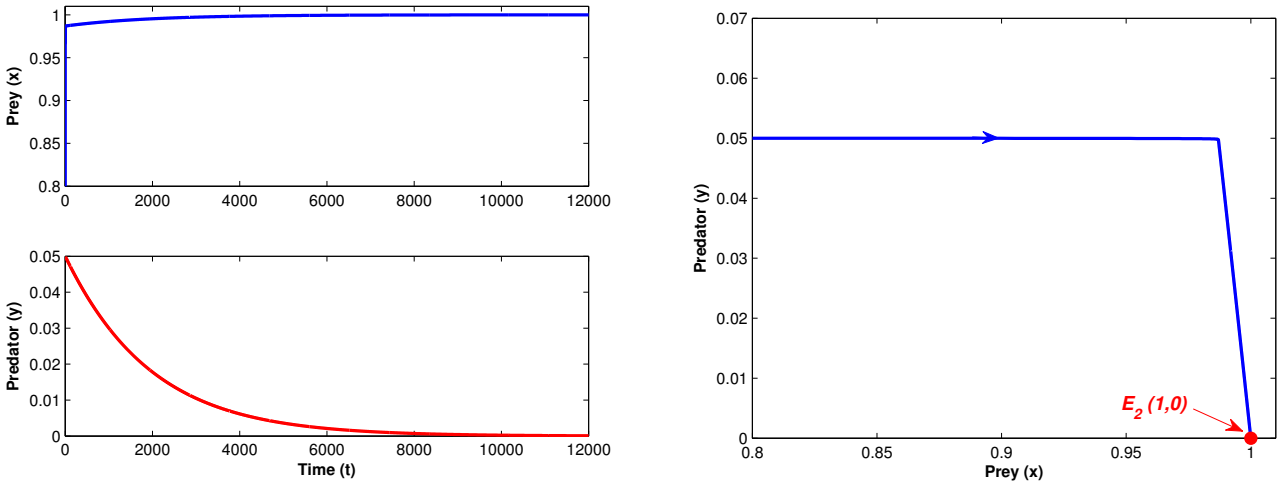

(18.a) *(18.b)*

Figure 18: Stable behaviour of E_2 in system (2.4) for $\eta = 0.017$.

In presence of specialist predator also, from the steady state situation of $E_2(1, 0)$, if the anti-predation rate starts to decrease, then at some threshold value of $\eta = \eta_{[TC_2]}$, E_2 loses its stability and becomes unstable once η lies below $\eta_{[TC_2]}$. So, system (2.4) undergoes a transcritical bifurcation around E_2 at $\eta = \eta_{[TC_2]} = 0.016462$ (see Figure 19).

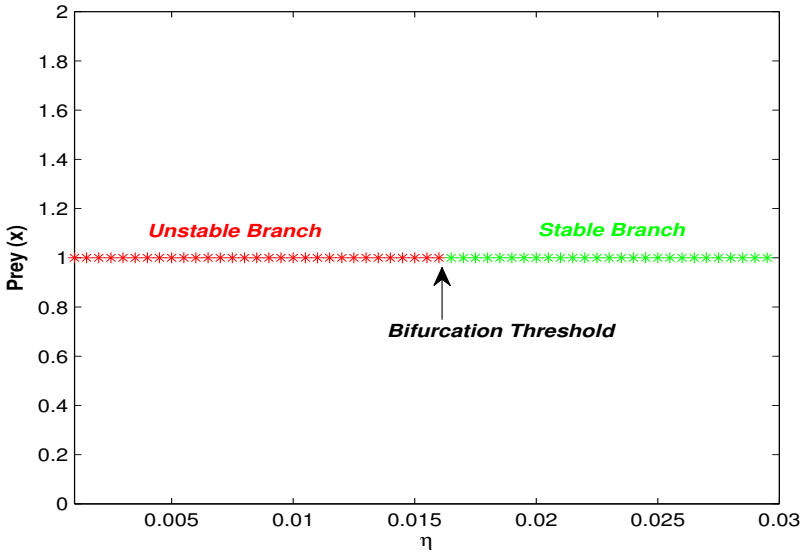

Figure 19: Transcritical Bifurcation around E_2 in system (2.4) taking η as bifurcation parameter.

One of the interesting dynamics which is observed in system (2.4) is occurrence of tristability. For the parametric values in Table 4 along with $\eta = 0.017$, it is observed that any trajectory can converge to either $E_0(0, 0)$ or $E_2(1, 0)$ or $E^*(0.59, 0.79)$. Choice of initial point is important in this case. For example, trajectories starting from $(0.25, 0.45)$ and $(0.2, 0.2)$ approach to E_0 and E_2 respectively. Again trajectories starting from $(0.55, 0.76)$ and $(0.53, 0.78)$ approach to E^* and from $(0.55, 0.6)$ approaches to E_2 (see Figure 20).

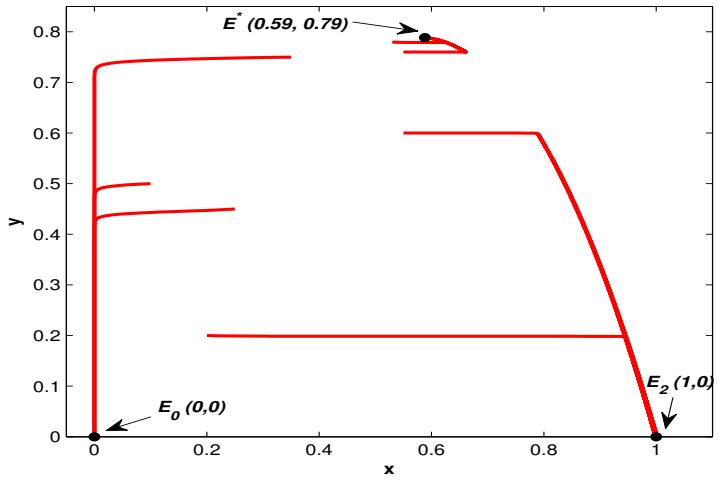

Figure 20: Tristable behaviour between E_0, E_2 and E^* of system (2.4) for $\eta = 0.017$.

If we look at Figure 21, it can be observed that there is a very small region where the feasible interior equilibrium point be stable. For $p = 0.1$, the interior point be feasible as well as stable only when $\eta \in [0.016995, 0.017010]$. We get a very small basin of attraction of E^*. A slight perturbation in initial point can

lead the system to converges to either E_0 or E_2 instead of E^*.

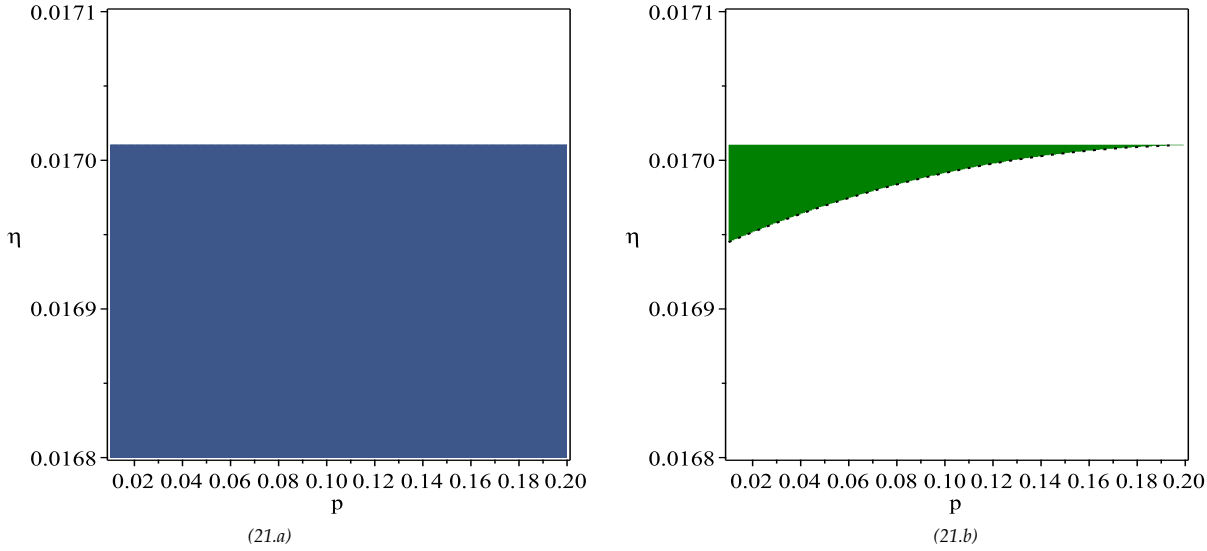

Figure 21: In system (2.4): (21.a) Feasible region of interior point E^*; (21.b) Stable region of interior point E^*.

Figure 22 helps us to detect the Hopf, saddle-node and transcritical bifurcation thresholds in one figure. This figure depicts that at $\eta_{[TC_3]} = 0.0033009739$, a transcritical bifurcation occurs around E^* and interior point actually generates from this point with coordinates $(0.1, 0)$ (denoted by "BP_2"). Increasing value of η gives unstable equilibrium point for $\eta_{[TC_3]} < \eta < \eta_{[H]}$. But in $\eta_{[H]} < \eta < \eta_{[sn]}$, we get stable equilibrium point. So, at $\eta = \eta_{[H]} = 0.016991478$, the system undergoes a Hopf bifurcation (denoted by "H") and we get a stable situation from oscillating state when η exceeds $\eta_{[H]}$. In fact, oscillating behaviour around E^* is observed only when $\eta \in (0.0169912, 0.016991478)$. Figure 23 show that at $\eta = 0.0169914$, system (2.4) performs oscillating behaviour and a stable limit cycle occurs around the unstable equilibrium point $E^*(0.576, 0.789)$ (1^{st} Lyapunov exponent, $l_1 = -6.747277e^{+00} < 0$)). As l_1 is negative, so, the Hopf bifurcation is supercritical.

Further at $\eta = \eta_{[sn]} = 0.017011$, the system undergoes a saddle-node bifurcation around E^* (denoted by "LP"). For $\eta > \eta_{[sn]}$, there does not exist any feasible interior equilibrium point but when η lies below $\eta_{[sn]}$, there are two interior points. One branch is stable for $(\eta_{[H]}, \eta_{[sn]})$ and other branch is unstable for $(\eta_{[sn]}, \eta_{[TC_2]})$ and Figure 24 depicts the scenario. At $\eta_{[TC_2]} = 0.016462$, E^* coincides with $E_2(1, 0)$ and another transcritical bifurcation occurs (denoted by "BP_1"). It is described in Figure 19 also.

It is noted that, m represents m_1 in Figure 25 and Figure 26. (η, m_1) and (η, p) have been taken as the bifurcation parameters to analyse the two-dimensional bifurcation. Bogdanov-Takens and Cusp bifurcation are observed in various cases. "BT" represents Bogdaonov-Takens bifurcation and "BT" bifurcation occurs at the intersection of saddle-node and Hopf curve. Taking (η, p) as bifurcation parameters, system (2.4) undergoes BT bifurcation at $(\eta_{[BT_1]}, p_{[BT_1]}) = (0.017011, 0.213065)$ with the equilibrium component $(0.63, 0.61)$ (see Figure (25.a)). Here the normal form coefficients are $(a, b) = (4.153738e^{-04}, -1.264405e^{+00})$. Further, another BT bifurcation can be observed at η-m_1 plane taking these two as bifurcation parameters where the bifurcation thresholds are $(\eta_{[BT_2]}, m_{1[BT_2]}) = (0.020107, 0.345677)$ with the equilibrium component $(0.575816, 0.684741)$ (see Figure (25.b)). The normal form coefficients are $(a, b) = (-5.977896e^{-04}, 1.166842e^{+00})$.

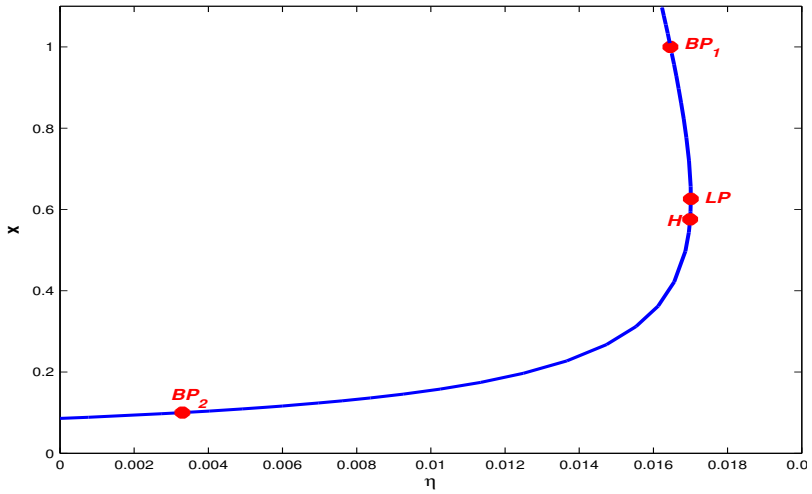

Figure 22: Bifurcations in system (2.4) taking η as bifurcation parameters. BP_1, BP_2 : Transcritical bifurcations, H : Hopf bifurcation, LP : Saddle-node bifurcation.

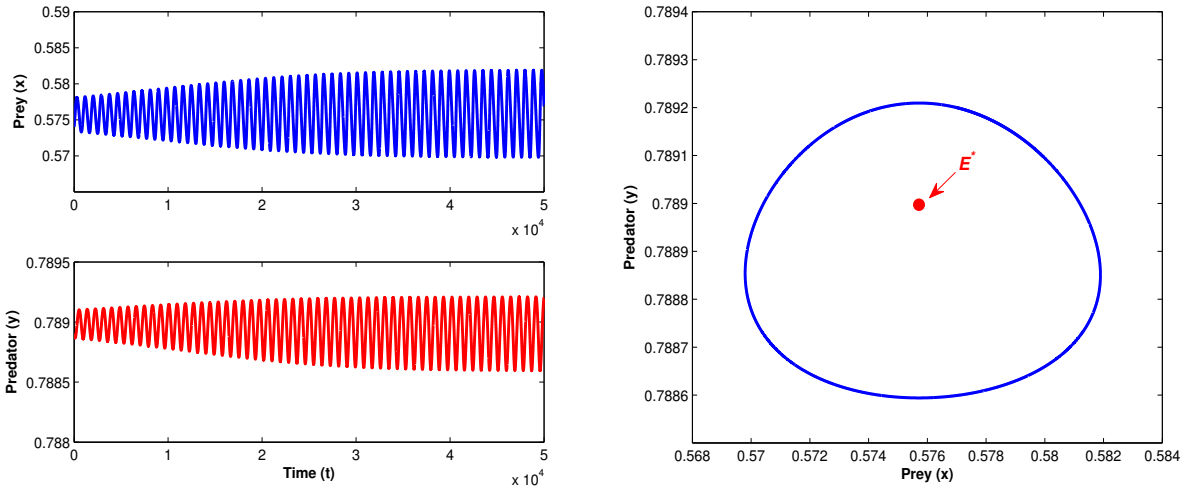

(23.a) (23.b)

Figure 23: Oscillating behaviour and occurrence of stable limit cycle in system (2.4) for $\eta < \eta_{[H]}$.

Except "BT" bifurcation, another two dimensional bifurcation is observed in this model which is cusp bifurcation. Taking (η, m_1) as bifurcation parameters, Figure 26 depicts that at $(\eta_{[CP]}, m_{1[CP]}) = (0.006668, 0.140860)$, system (2.4) undergoes a non-degenerate cusp bifurcation with equilibrium component $(0.999876, 0.001034)$ and the normal form coefficient is $c = -2.200932e^{-05}$). Also, a "BT" point in this figure indicates occurrence of BT bifurcation and it is elaborated in Figure (25.b).

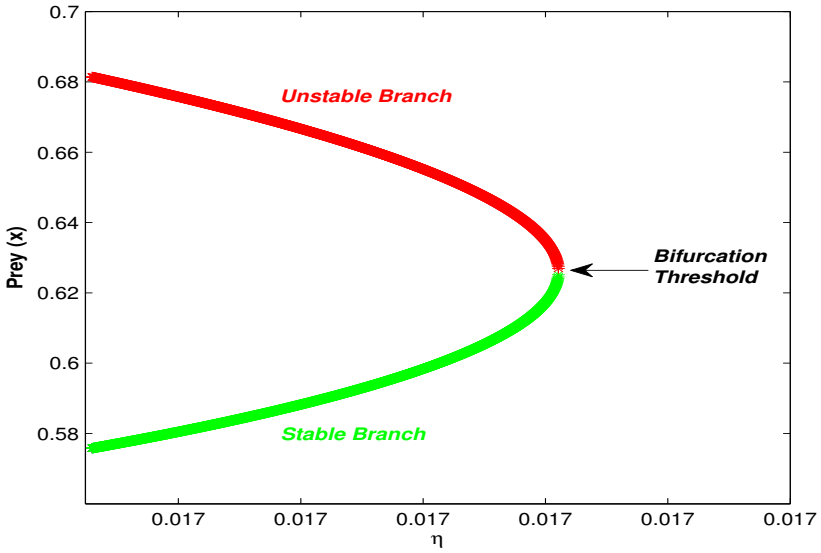

Figure 24: Saddle-node Bifurcation around E^* in system (2.4) taking η as bifurcation parameter.

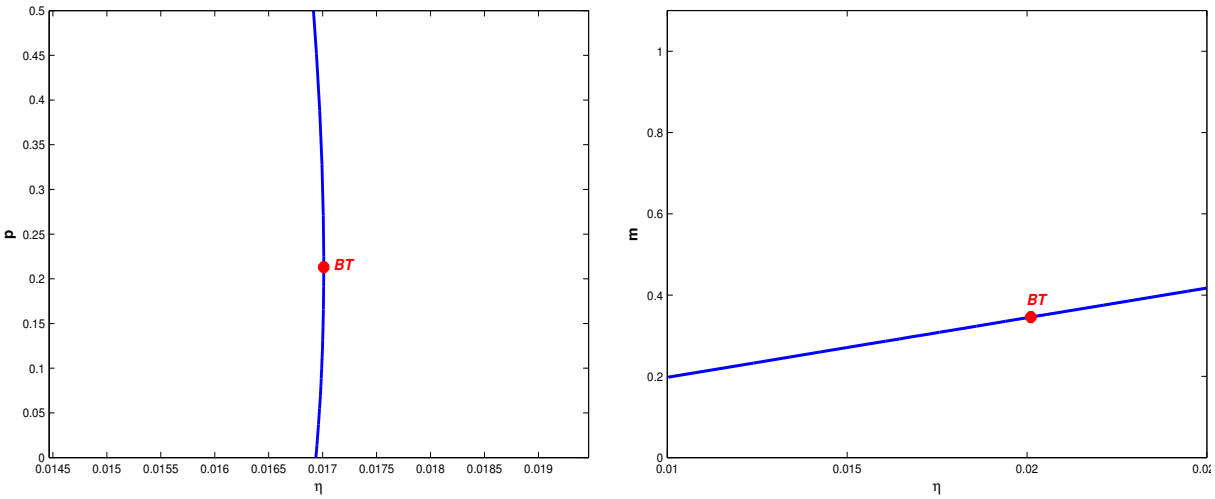

(25.a) (25.b)

Figure 25: In system (2.4), two parameter Bogdanov-Takens bifurcation diagrams: (25.a) in η-p plane where $BT \equiv \left(\eta_{[BT_1]},\ p_{[BT_1]}\right)$; (25.b) in η-m_1 plane where $BT \equiv \left(\eta_{[BT_2]},\ m_{1[BT_2]}\right)$.

■ Impact of anti-predator behaviour

(a) on generalist predator: Figure 27 depicts the trajectory profiles of prey (x) and predator (y) population of system (2.2) for increasing value of η. It is observed that the prey population increases when η starts to increase but the slope of the curve is not at all sharp. Prey population is always at a higher density irrespective of any anti-predation rate. Now if we look at the trajectory for the predator population, then it is found to be a monotonically decreasing curve with increasing anti-predation rate. If the prey starts to hunt the juvenile predator or prey harm the predator at a higher rate, then ultimately the predator decrease.

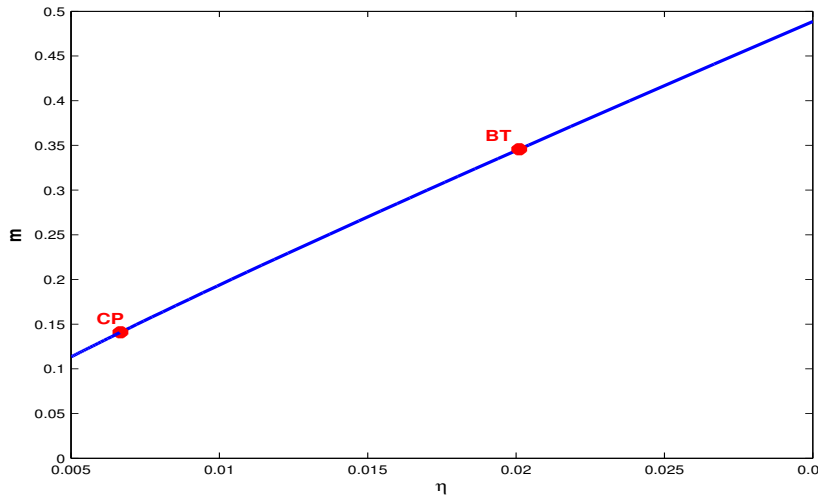

Figure 26: In system (2.4), two parameter bifurcation diagrams in η-m_1 plane: Cusp bifurcation where $CP \equiv \left(\eta_{[CP]},\ m_{1[CP]}\right)$ and Bogdanov-Takens bifurcation where $BT \equiv \left(\eta_{[BT_2]},\ m_{1[BT_2]}\right)$.

The slope of the trajectory is not so steep.

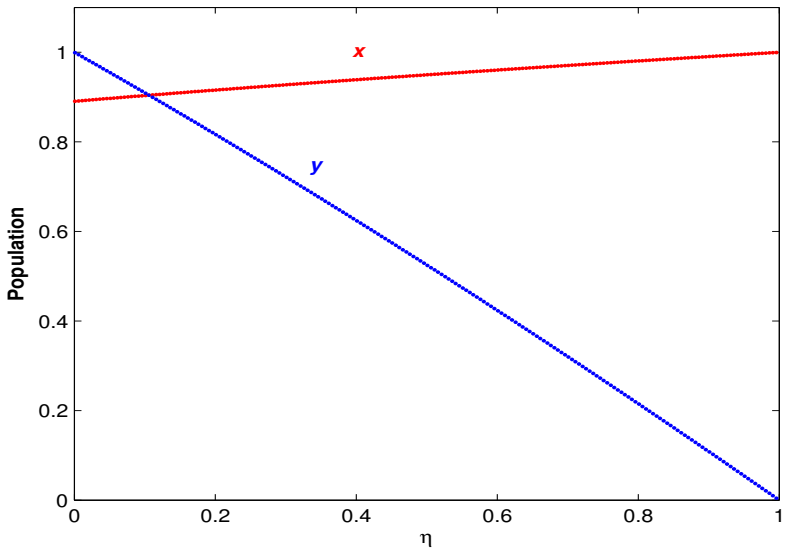

Figure 27: Trajectory profiles of system (2.2) for increasing anti-predation rate (η). Here $p = 0.17, m = 0.5,\ a = 6,\ r = 1$.

(b) on specialist predator: Figure 28 depict the trajectory profiles of prey (x) and predator (y) of system (2.4) for increasing value of η in presence of specialist predator. Here also the prey population increases with increasing η but the rate of increment is higher than the previous case. On the other hand, the predator population first increases then decreases with increasing anti-predation rate. But the rate of increment, as well as decrement, is very slow. If the prey counter-attack the predator with a very small rate, then it does not affect the predator's growth and the predator population increases. But if the anti-predation rate

continuously increases, then ultimately predator population starts to decrease. So, the trajectory profile of predator population first increases then decreases for increasing anti-predation rate of prey species. When η starts to increase, then after crossing a range, predator starts to decrease.

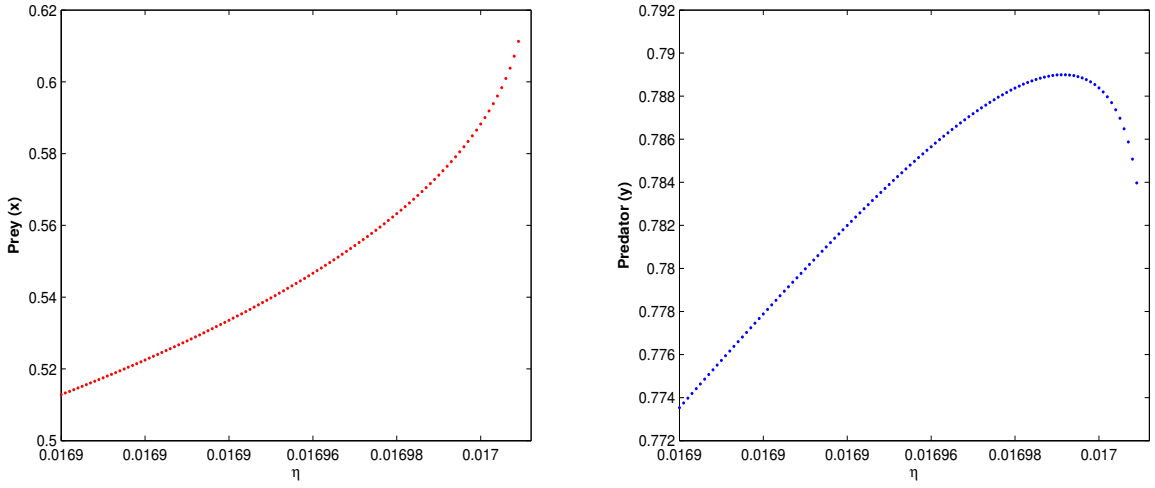

(28.a) *(28.b)*

Figure 28: Trajectory profiles of system (2.4) for increasing anti-predation rate (η). Here $p = 0.1, m_1 = 0.3, a = 0.3, c = 0.08, d = 0.002$.

9. Discussion

Anti-predator behaviour is a natural phenomenon which is observed in the prey population when they start to fight back to save themselves from predator's attack. In some cases prey only try to avoid the predation while in some cases prey in fact attack and kill predator by applying different defence strategies. So, it is quite obvious that a certain amount of prey is needed to apply the anti-predator strategy. In this paper, a simple prey-predator model has been considered where the prey population exhibits anti-predator behaviour. Also, a strong Allee effect in prey population ensures that a certain amount of prey population is needed for a positive growth rate. Positivity and boundedness of the system variables of both proposed systems ensure that the systems are biologically well-defined. The first interesting thing which is observed that the trivial equilibrium point E_0 acts always as a saddle point when the predator population is considered to be a generalist one. But in the presence of a specialist predator, E_0 becomes a stable point for any parametric values. This is why the system with generalist predator shows bistability, i.e., for some assumed parametric values, a trajectory converges to either prey-free equilibrium E_3 or coexisting equilibrium E^* depending on the choice of the initial point. It means if a trajectory starts in the basin of attraction which contains E_3, then it ultimately converges to E_3 with time and if a trajectory starts in the region of attraction containing E^*, then it ultimately converges to E^* as time goes. Another bistability can be observed between predator-free equilibrium $E_2(1, 0)$ and coexisting state E^*. In this case also, a trajectory converges to either E_2 or E^* depending on the choice of the initial point. On the other hand, in the presence of a specialist predator, a situation of tri-stability can be observed. Here, a trajectory can converge to either E_0 or E_2 or even to E^* depending on the initial point.

Figures 20 and 21 show that the basin of attraction of E^* is very small. A slight perturbation in initial point can change the coexisting steady-state to population extinction or even predator-free state. Moreover, in presence of generalist predator, system (2.2) cannot exhibit any oscillating behaviour for any anti-predation rate, i.e., non-occurrence of the closed orbit is observed. But when the predator is assumed to be specialist, η plays a crucial role as a change in η can turn system (2.4) from steady-state situation to oscillation.

The impact of anti-predator behaviour on both systems has been analysed in section 10. In the presence of generalist predator, the predator population shows a monotonically decreasing curve while the prey population increases gradually. The graph suggests that the predator is at highest density when there is no anti-predation strategy is involved but it goes to extinction when the anti-predation rate exceeds its growth rate. Now, for the specialist predator, we observe a different scenario. The trajectory of predator population is monotonically increasing at an early stage but for comparatively higher value of anti-predation rate coefficient, it acts like a decreasing curve. This result implies that if the prey attacks the predator with a very small rate, then it does not affect the growth of predator species and they grow by consuming the prey population. But, if the prey starts to harm the predator with a higher rate, then ultimately after a threshold value of η, predator starts to decrease.

The analytical and numerical results prove that the proposed models exhibit rich dynamics but these can be refined further so that the models become more realistic to the environment. We may consider that the consumption term of predator not only as prey dependent but as predator dependent function too. Besides the consumption of food is not a process of a fraction of time; the predators take some time to digest the consumed food. Incorporation of 'gestation delay' will make the work more realistic. Besides, environmental fluctuations can also be incorporated into the model with the help of white noise to study the stochastic model. So, in future some models can be formulated considering all these facts to obtain different interesting results.

Conflict of Interest

The authors declare that they have no conflict of interest.

Acknowledgements

The authors are grateful to the anonymous referees, for their careful reading, valuable comments and helpful suggestions, which have helped them to improve the presentation of this work significantly. The first author (Sangeeta Saha) is thankful to the University Grants Commission, India for providing SRF.

References

[1] P. Abrams, H. Matsuda, Effects of adaptive predatory and anti-predator behaviour in a two-prey one-predator system, Evol. Ecol. 7 (1993) 312-326.
[2] L. Berec, E. Angulo, F. Courchamp, Multiple allee effects and population management, Trends Ecol. Evol. 22 (2006) 185-191.
[3] Y. Choh, M. Lgnacio, M.W. Sabelis, A. Janssen, Predator–prey role reversals, juvenile experience and adult antipredator behaviour, Sci Rep 2 (2012) 728. doi:10.1038/srep00728.
[4] F. Courchamp, L. Berec, J. Gascoigne, Allee Effects in Ecology and Conservation, Oxford University Press, Oxford, 2008.
[5] A. Cuspilici, P. Monforte, M.A. Ragusa, Study of Saharan dust influence on PM 10 measures in Sicily from 2013 to 2015, Ecological Indicators 76 (2017) 297–303. doi:10.1016/j.ecolind.2017.01.016
[6] L.W. Deng, X.D. Wang, M. Peng, Hopf bifurcation analysis for a ratio-dependent predator-prey system with two delays and stage structure for the predator, Appl Math Comput 231 (2014) 214-230.
[7] A. Duro, V. Piccione, M.A., Ragusa, V. Veneziano, New enviromentally sensitive patch index–ESPI–for MEDALUS protocol, AIP Conference Proceedings, vol.1637 (2014) 305-312. doi:10.1063/1.4904593
[8] F. Favreau, A.W. Goldizen, O. Pays, Interactions among social monitoring, anti-predator vigilance and group size in eastern grey kangaroos, Proc. Roy. Soc. B-Biol. Sci. 277 (2010) 2089-2095.
[9] J.K.B. Ford, R.R. Reeves, Fight or flight: Anti-predator strategies of baleen whales, Mamm. Rev. 38 (2008) 50-86.
[10] D. Ge, D. Chesters, J. Gómez-Zurita, L. Zhang, X. Yang, A.P. Vogler Anti-predator defence drives parallel morphological evolution in flea beetles, Proc. Roy. Soc. B-Biol. Sci. 278 (2011) 2133-2141.
[11] J.K. Hale, Theory of functional Differential Equations, Springer-Verlag, Heidelberg, 1977.
[12] A.R. Ives, A.P. Dobson, Antipredator behaviour and the population dynamics of simple predator-prey systems, Am Nat 130(3) (1987) 431-447.
[13] A. Janssen, F. Faraji, T. van der Hammen, S. Magalhães, M.W. Sabelis, Interspecific infanticide deters predators, Ecol Lett 5 (2002) 490-494.
[14] K.A. Jones, J.G.J. Godin, Are fast explorers slow reactors? Linking personality type and antipredator behaviour, Proc. Roy. Soc. B-Biol. Sci. 277 (2010) 625-632.
[15] K. Kiss, S. Kovács, Qualitative behavior of n-dimensional ratiodependent predator-prey system, Appl Math Comput 199 (2008) 535-546.
[16] M. Kot, Elements of Mathematical Biology, Cambridge University Press, Cambridge, 2001.

[17] C. Lai, A. Smith, Keystone status of plateau pika (*Ochotona curzoniae*): Effect of control on biodiversity of native birds, Biodivers. Conserv. 12 (2003) 1901-1912.
[18] S.L. Lima, Stress and decision-making under the risk of predation: recent developments from behavioral, reproductive, and ecological perspectives, Adv Study Behav 27 (1998) 215-290.
[19] S. Lingle, S.M. Pellis, Fight or flight? Anti-predator behavior and the escalation of coyote encounters with deer, Oecologia 131 (2002) 154-164.
[20] X.N. Liu, L.S. Chen, Complex dynamics of Holling type II Lotka-Volterra predator-prey system with impulsive perturbations on the predator, Chaos Solitons Fractals 16 (2003) 311-320.
[21] J. Murray, Mathematical Biology (ii): Spatial models and biomedical applications (3^{rd} edition), 2003.
[22] A. Pallini, A. Jaassen, M.W. Sabelis, Predators induce interspecific herbivore competition for food in refuge space, Ecol Lett 1 (1998) 171-177.
[23] M. Perc, P. Grigolini, Collective behavior and evolutionary games-An introduction, Chaos Solitons Fractals 56 (2013) 1-5.
[24] L. Perko, Differential Equations and Dynamical Systems, Springer-Verlag, New York, 2001.
[25] V. Piccione, M.A. Ragusa, V. Rapicavoli, V. Veneziano, Monitoring of a natural park through ESPI, AIP Conference Proceedings, vol.1978 art.n. 140005 (2018). doi:10.1063/1.5043785
[26] R. Ramos-Jiliberto, E. Frodden, A. Aŕanguiz-Acuña, Pre-encounter versus post-encounter inducible defenses in predator-prey model systems, Ecol. Model. 200(1-2) (2007) 99-108.
[27] R.A. Relyea, How prey respond to combined predators: a review and an empirical test, Ecology 84 (2003) 1827-1839.
[28] Y. Saitō, Prey kills predator: counter-attack success of a spider mite against its specific phytoseiid predator, Exper Appl Acarol 2 (1986) 47-62.
[29] Y. Shi, On the influences of range land vegetation to the density of plateau pika (*Ochotona curzoniae*), Acta Theriol. Sin. 3 (1983) 181-187.
[30] A.T. Smith, J.M. Foggin, The plateau pika (Ochotona curzoniae) is a keystone species for biodiversity on the Tibetan plateau, Anim. Conserv. 2 (1999) 235-240.
[31] P.A. Stephens, W.J. Sutherland, R.P. Freckleton, What is the Allee effect? Oikos 87 (1999) 185-190.
[32] M. Stevens, W.T.L. Searle, J.E. Seymour, K.L.A. Marshall, G.D. Ruxton, Motion dazzle and camouflage as distinct anti-predator defenses, BMC Biol. 9 (2011) 81. doi: 10.1186/1741-7007-9-81.
[33] X. Sun, Y. Li, Y. Xiao, A Predator–Prey Model with Prey Population Guided Anti-Predator Behavior, International Journal of Bifurcation and Chaos 27(07) (2017) 1750099. doi:10.1142/s0218127417500997
[34] A. Szolnoki, M. Mobilia, L.L. Jiang, B. Szczesny, A.M. Rucklidge, M. Perc, Cyclic dominance in evolutionary games: a review, J R Soc Interface 11 (2014) 20140735.
[35] S.Y. Tang, J.H. Liang, Global qualitative analysis of a non-smooth Gause predator–prey model with a refuge, Nonlinear Anal TMA 76 (2013) 165-180.
[36] B. Tang, Y. Xiao, Bifurcation analysis of a predator-prey model with anti-predator behaviour, Chaos Solit. Fract. 70 (2015) 58-68.
[37] R. Tolrian, Predator-included morphological defenses: costs, life history shifts, and maternal effects in Daphnia pulex, Ecology 76 (1995) 1691-1750.
[38] J. Wang, J. Shi, J. Wei, Predator-prey system with strong Allee effect in prey, J. Math. Biol. 62 (2011) 291-331.
[39] G. Wang, X.G. Liang, F.Z. Wang, The competitive dynamics of populations subject to an Allee effect, Ecol. Model. 124 (1999) 183-192.
[40] M.H. Wang, M. Kot, Speeds of invasion in a model with strong or weak Allee effects, Math. Biosci. 171 (2001) 83-97.
[41] X. Wang, X. Fu, Sustainable management of alpine meadows on the Tibetan Plateau: Problems overlooked and suggestions for change, Ambio 33 (2004) 169-171.
[42] X. Wei, S. Li, P. Yang, H. Cheng, Soil erosion and vegetation succession in alpine Kobresia steppe meadow caused by plateau pika-A case study of Nagqu County, Tibet, Chinese Geographical Science 17 (2007) 75-81.
[43] X.Q. Zhao, X.M. Zhou, Ecological basis of alpine meadow ecosystem management in Tibet : Haibei Alpine Meadow Ecosystem Research Station, Ambio 28(8) (1999) 642-647.
[44] H. Zhou, L. Zhou, X. Zhao, W. Liu, Y. Li, S. Gu, X. Zhou, Stability of alpine meadow ecosystem on the Qinghai-Tibetan Plateau, CHINESE SCI BULL 51 (2006) 320-327. doi:10.1007/s11434-006-0320-4.
[45] W.J. Zuo, Global stability and Hopf bifurcation of a Beddington–DeAngelis type predator-prey system with diffusion and delays, Appl Math Comput 223 (2013) 423-435.